

# Precision Physics and Antimatter

**Part 5 – Antiproton(ic) CPT invariance tests**

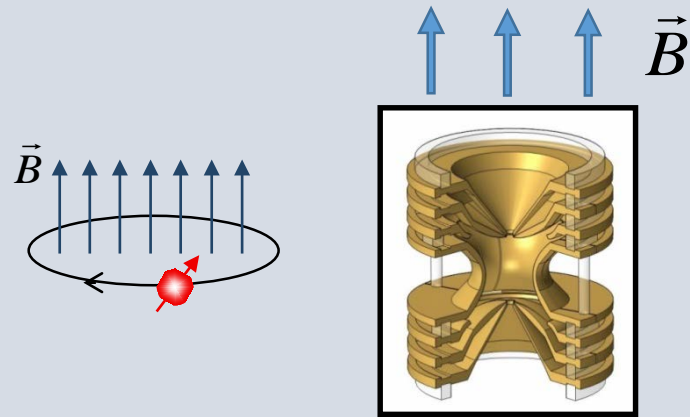
Dr. Andreas Mooser and Dr. Christian Smorra

39th Graduate Days  
Ruprecht-Karls-Universität Heidelberg

# Summary on precision magnetic moment measurements

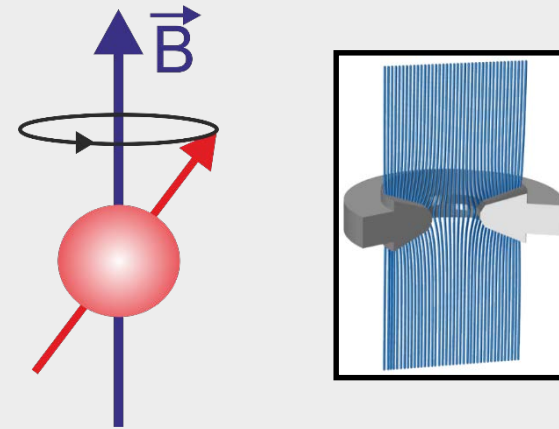
# High-precision measurements in Penning traps

## Cyclotron Frequency



$$\omega_c = \frac{q}{m} B$$

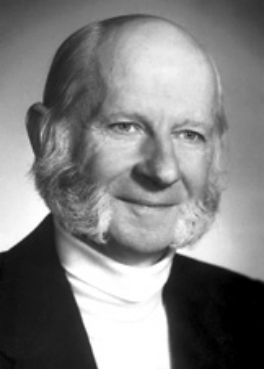
## Larmor Frequency



$$\omega_L = g \frac{e}{2m_p} B$$

$$\frac{\omega_{c,\bar{p}}}{\omega_{c,p}} = \frac{q_{\bar{p}}/m_{\bar{p}}}{q_p/m_p}$$

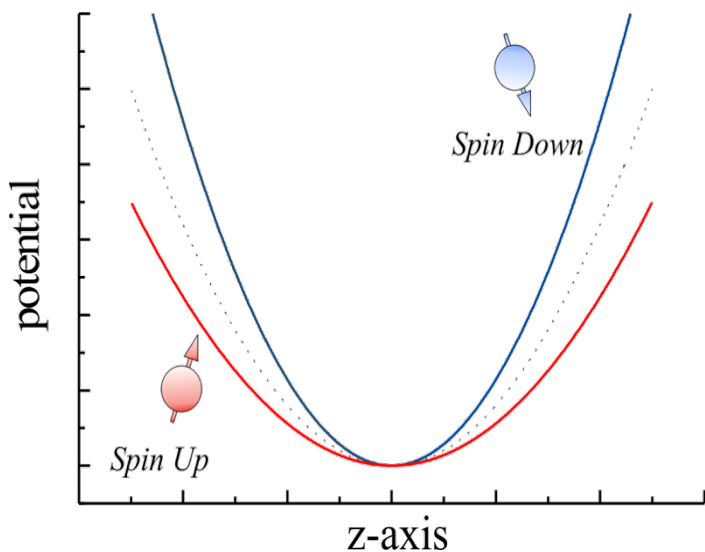
$$\frac{\omega_L}{\omega_c} = \frac{g}{2} = \frac{\mu}{\mu_N}$$



# How to measure the Larmor frequency? The continuous Stern-Gerlach effect

Introduce magnetic inhomogeneity, the magnetic bottle

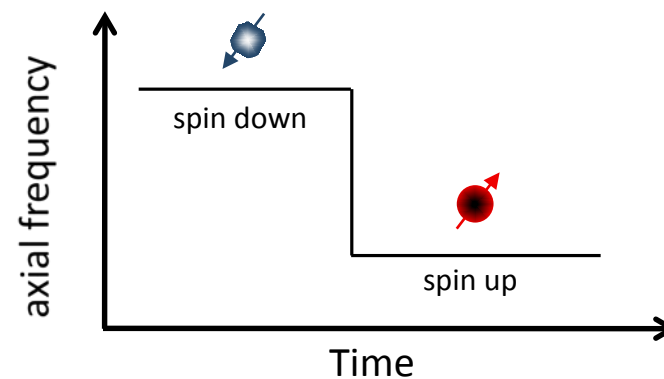
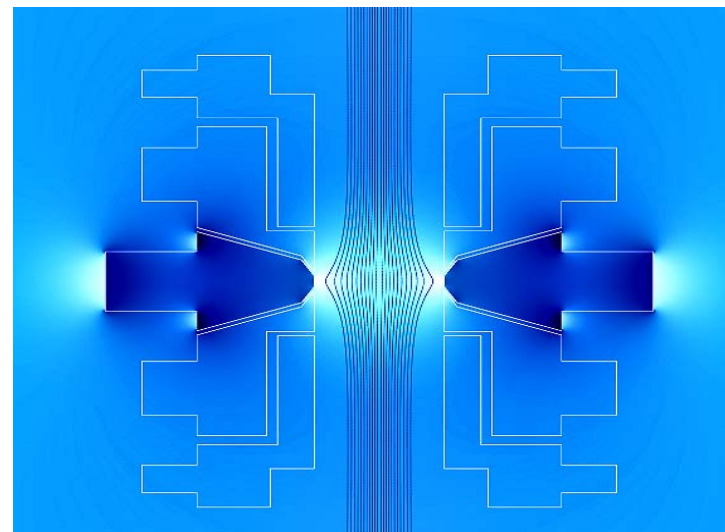
$$B_z = B_0 + B_2 \left( z^2 - \frac{\rho^2}{2} \right)$$



$$\Phi_z = \pm \mu_p B_z$$

Spin flip results in shift of the axial frequency

$$\nu_z \propto \frac{\mu_p}{m} B_2$$



# Electron g-Faktor and QED

- Effects described by Schwinger series

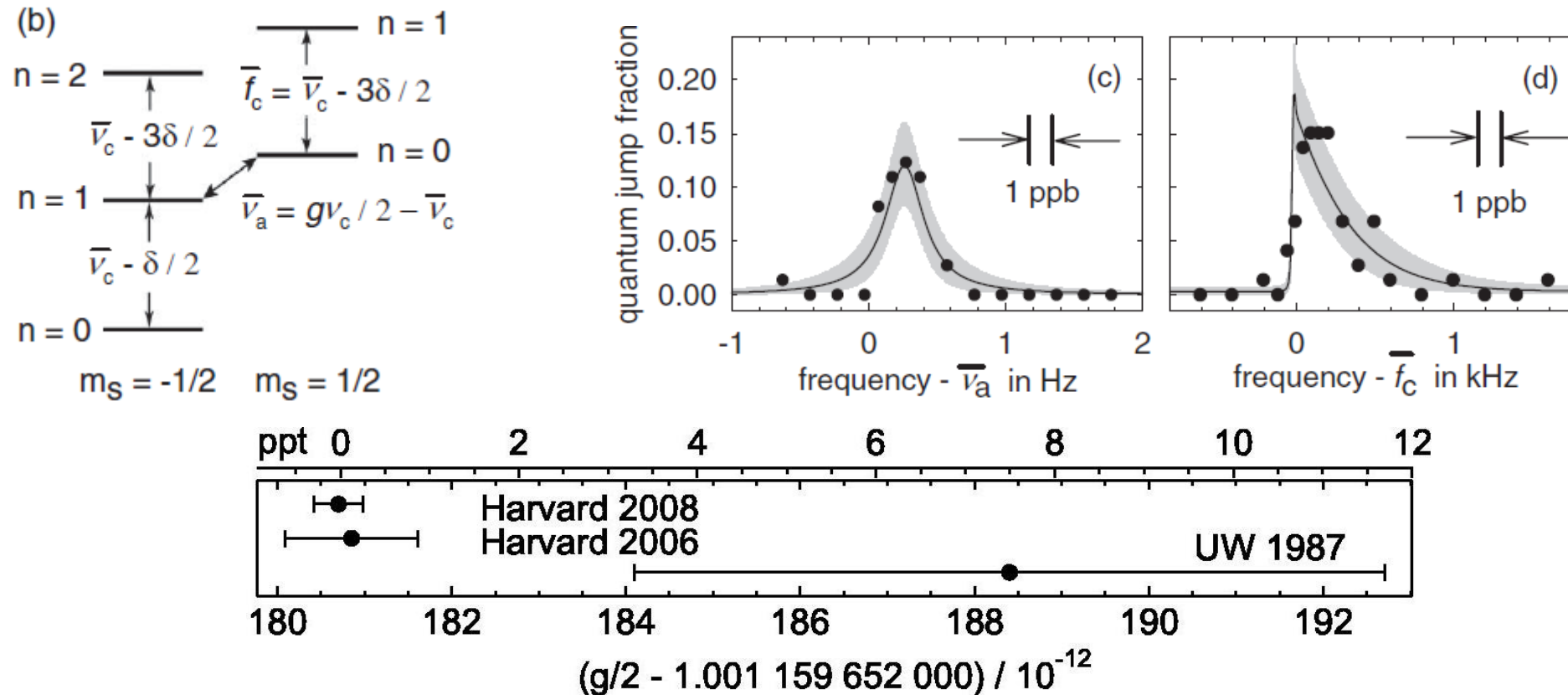
$$\frac{g}{2} = 1 + C_2 \left( \frac{\alpha}{\pi} \right) + C_4 \left( \frac{\alpha}{\pi} \right)^2 + C_6 \left( \frac{\alpha}{\pi} \right)^3 + C_8 \left( \frac{\alpha}{\pi} \right)^4 + \dots$$
$$+ a_{\mu\tau} + a_{\text{hadronic}} + a_{\text{weak}},$$

C <sub>2</sub>	0,5
C <sub>4</sub>	-0,328478965579
C <sub>6</sub>	1,181241456587
C <sub>8</sub>	-1,9144(35)
a <sub>μ,τ</sub>	2,720919(3) 10 <sup>-12</sup>
a <sub>hadronic</sub>	1,682(20) 10 <sup>-12</sup>
a <sub>weak</sub>	0,0297(5) 10 <sup>-12</sup>

$$a_e(\text{theo}) = \frac{g - 2}{2} = 0,00115965218113 \text{ (84)}$$

10<sup>th</sup> order 12 672 diagrams  
calculated

# Single electron quantum jump spectroscopy



**No signature for new physics yet - Independent measurement of the fine structure constant is necessary**  
**CPT invariance test (g-2) measurement of the positron by Dehmelt - Best SME-limits for electrons**

# SME in a Penning trap I

SME reduces to

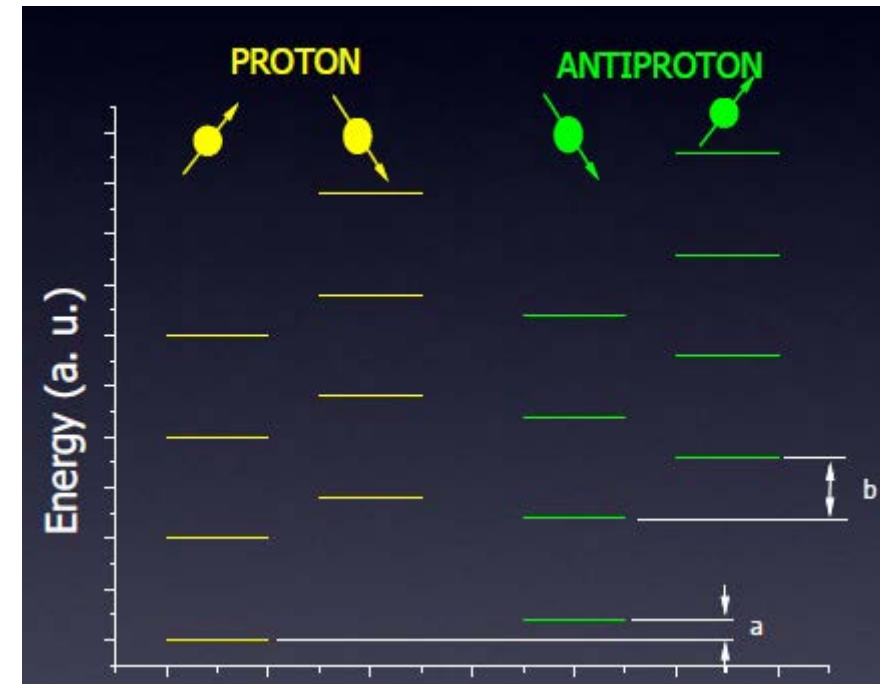
$$\left( i\gamma^\mu D_\mu - m - a_\mu \gamma^\mu - b_\mu \gamma^5 \gamma^\mu \right) \psi = 0$$

- a – shifts levels, no measurable effect in Penning trap
- b – modification of anomaly frequency

$$r_g = \frac{E_p - E_{\bar{p}}}{E_p} = \frac{\delta\omega_a}{m}$$

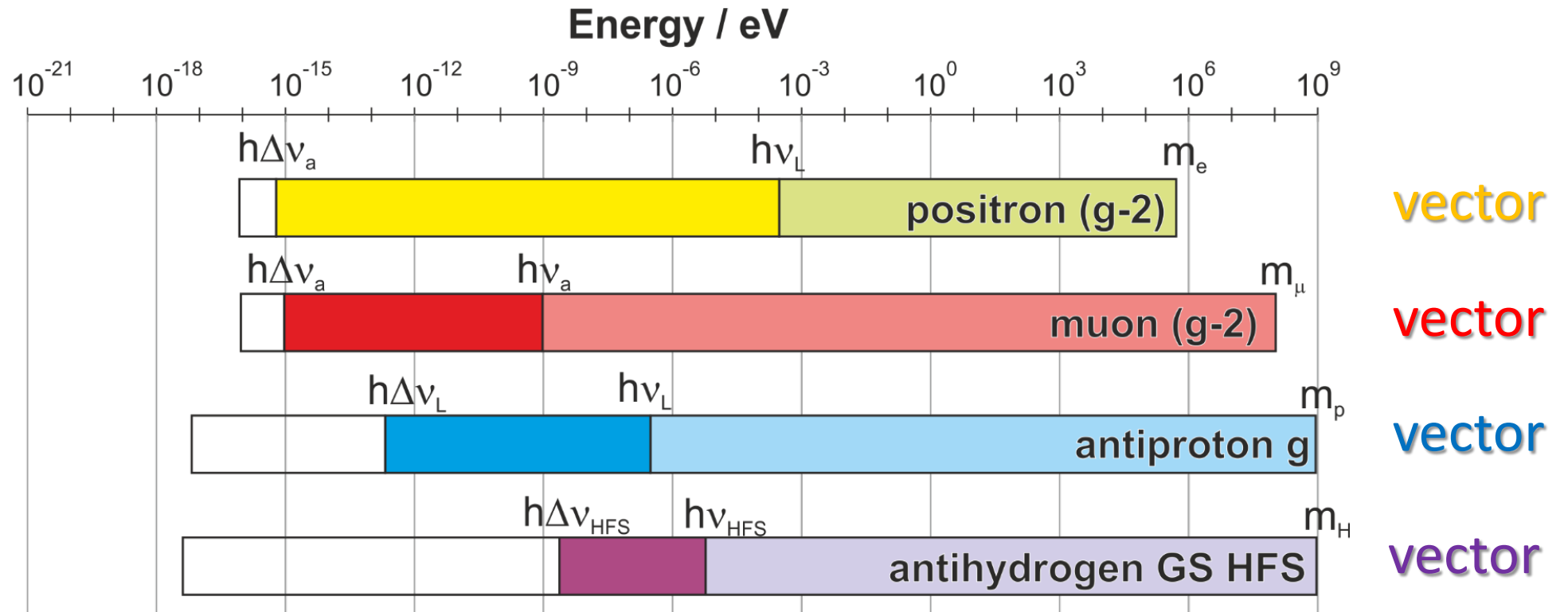
Electron

Positron



# Energy resolution of g-factor measurements

$$\frac{\delta E}{E} = \frac{h \Delta \nu}{m c^2}$$



4 very important tests for CPT-odd interactions

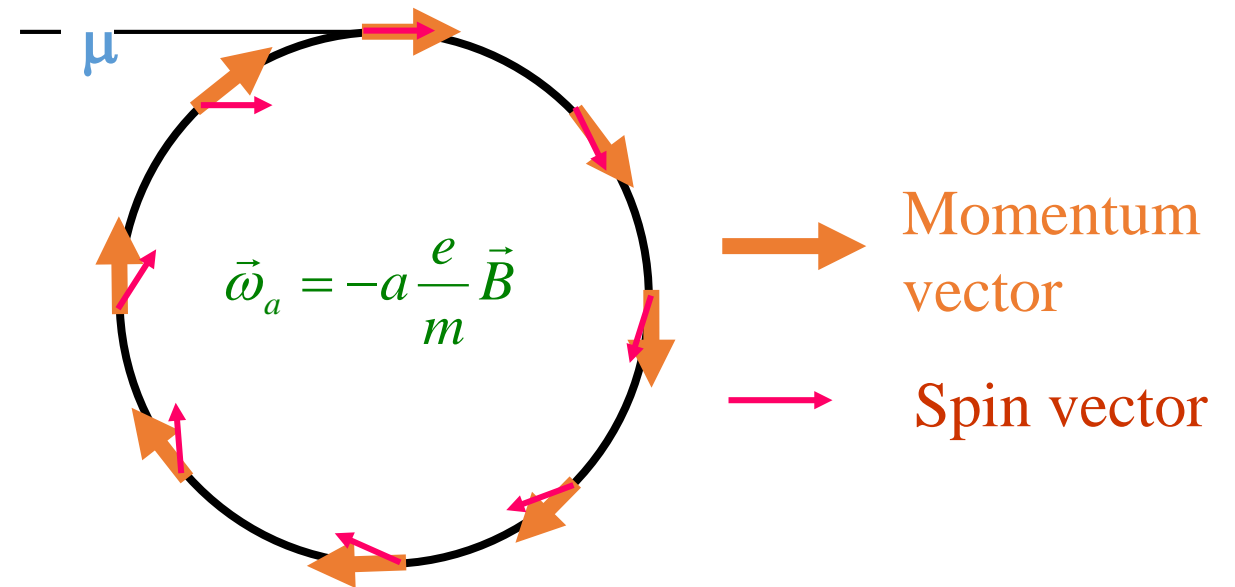
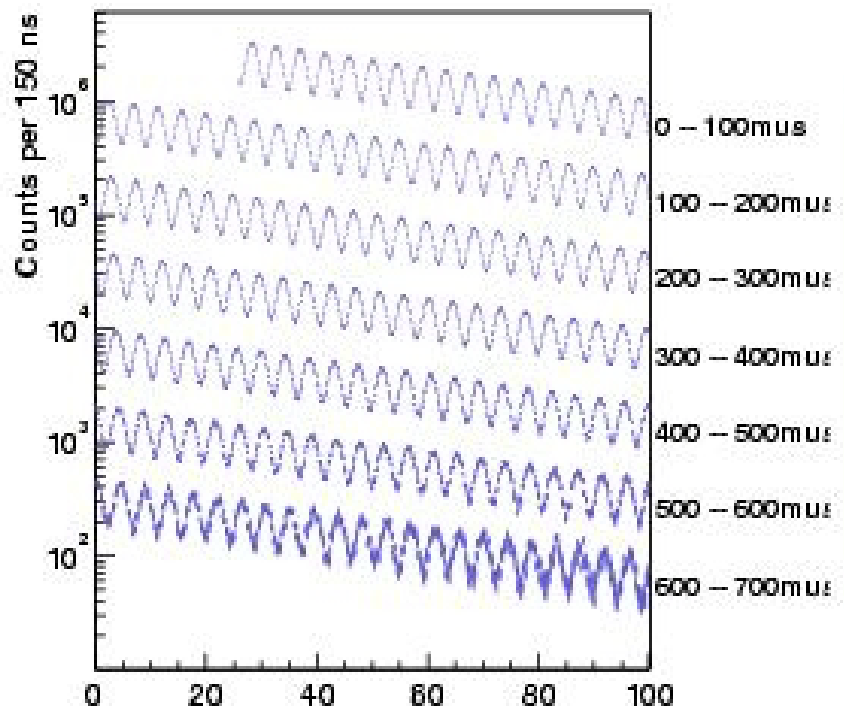
Think of CP-violation which exists only for a few mesons/exotic baryons

Need to search in all available systems



# Measurement of the muon magnetic moment

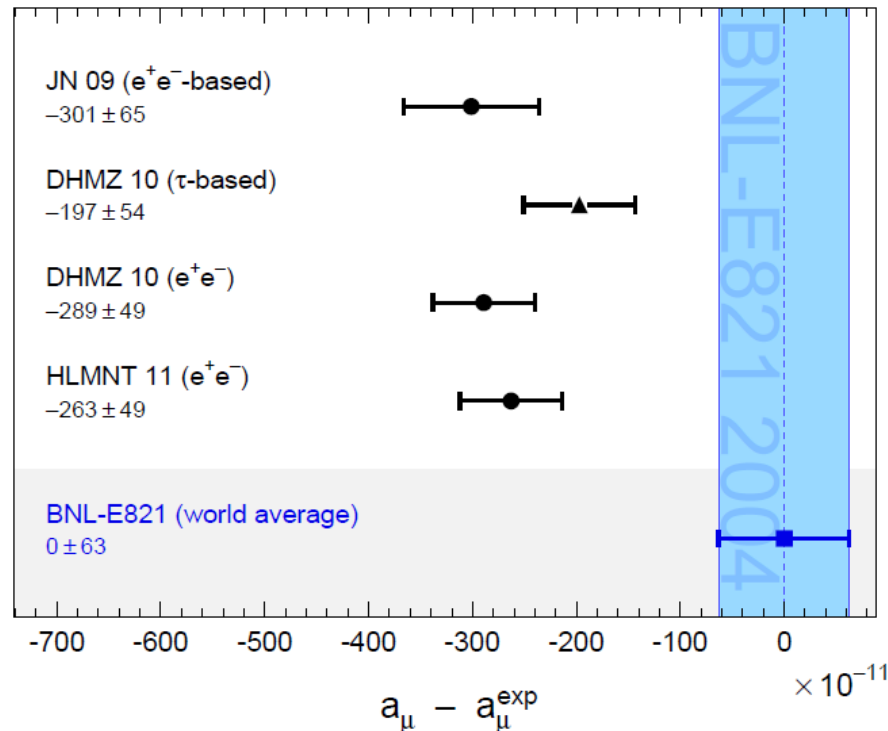
$$N(t) = N_0 e^{-\frac{t}{\gamma\tau}} \left[ 1 + A \cos(\omega_a t + \phi) \right]$$



# Muon magnetic anomaly and Helium-3

Muon and Antimuon are found to agree

But 3.6 Sigma discrepancy observed to theory



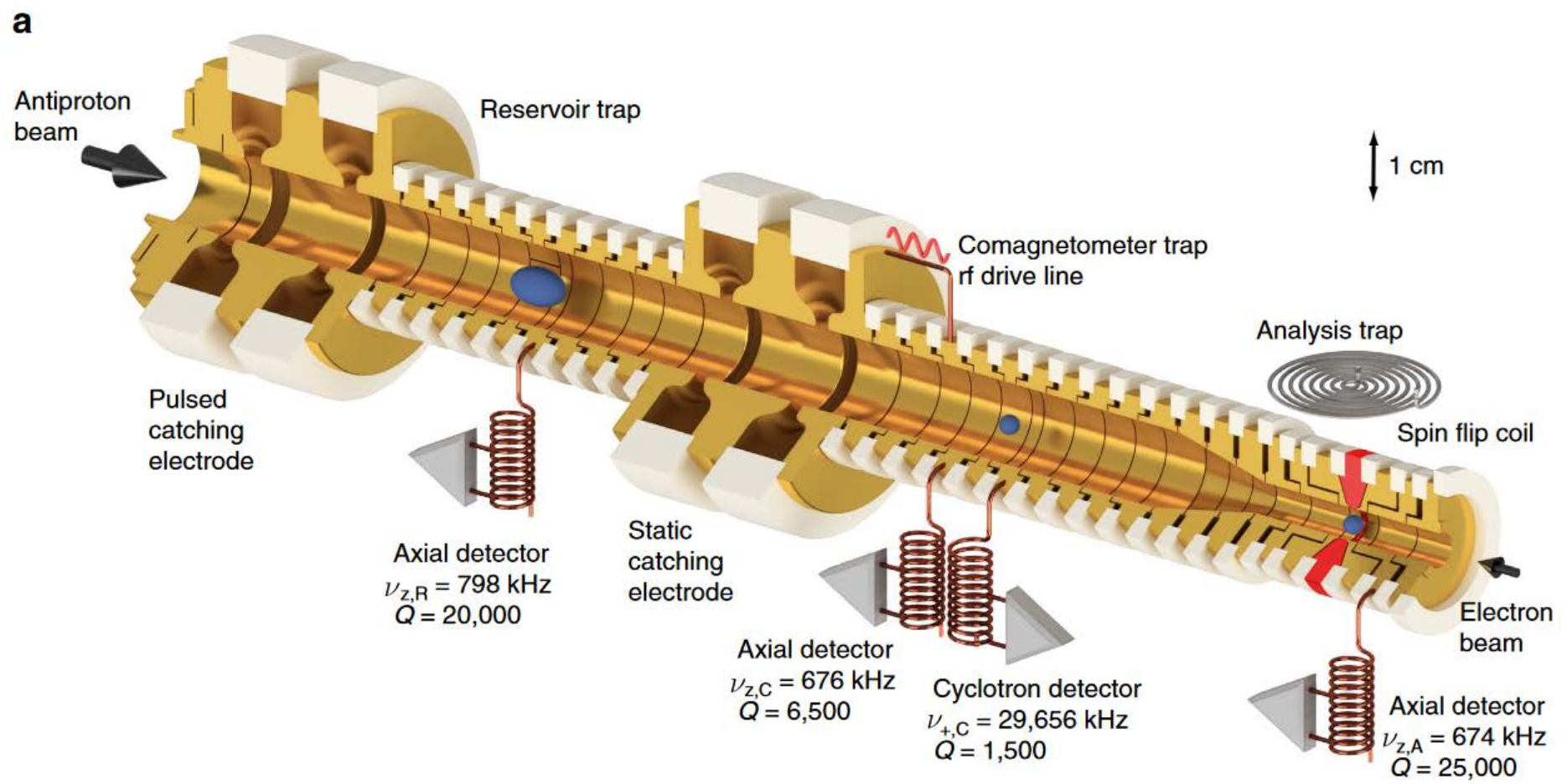
New measurement at Fermilab

$$a_{\mu} = \frac{g - 2}{2} = \frac{\omega_a / \omega_p}{\omega_L / \omega_p - \omega_a / \omega_p}$$

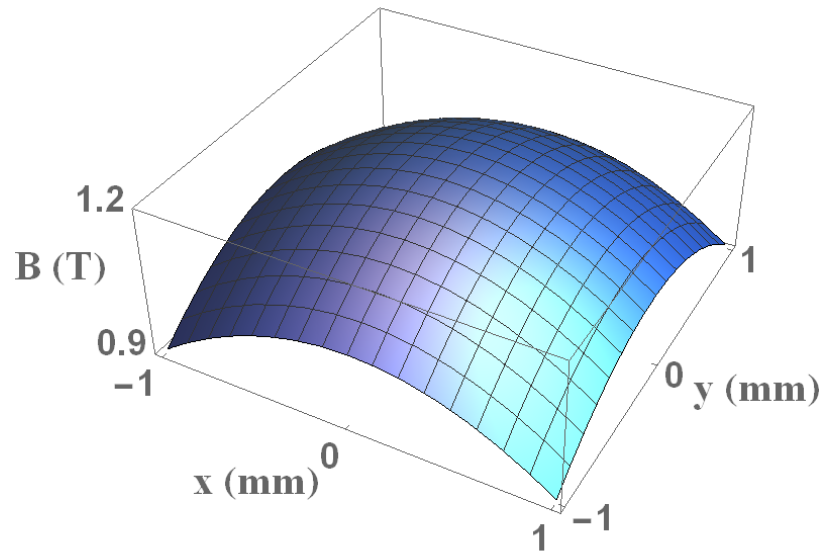
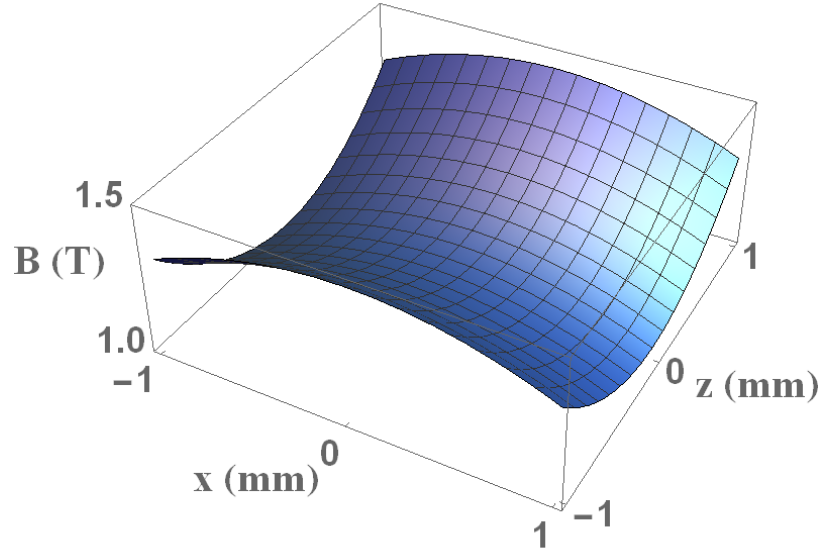
Muonium Hyperfine Splitting  
Museum Experiment @ J-PARC (Japan)

$$\frac{\omega_a}{\omega_p} = \frac{\omega_a \tilde{\omega}_p}{\tilde{\omega}_p \omega_p} \longleftrightarrow \frac{\omega_a}{\omega_p} = \frac{\omega_a}{\omega_{He-3}} \frac{\omega_{He-3}}{\omega_p}$$

# Antiproton magnetic moment measurement

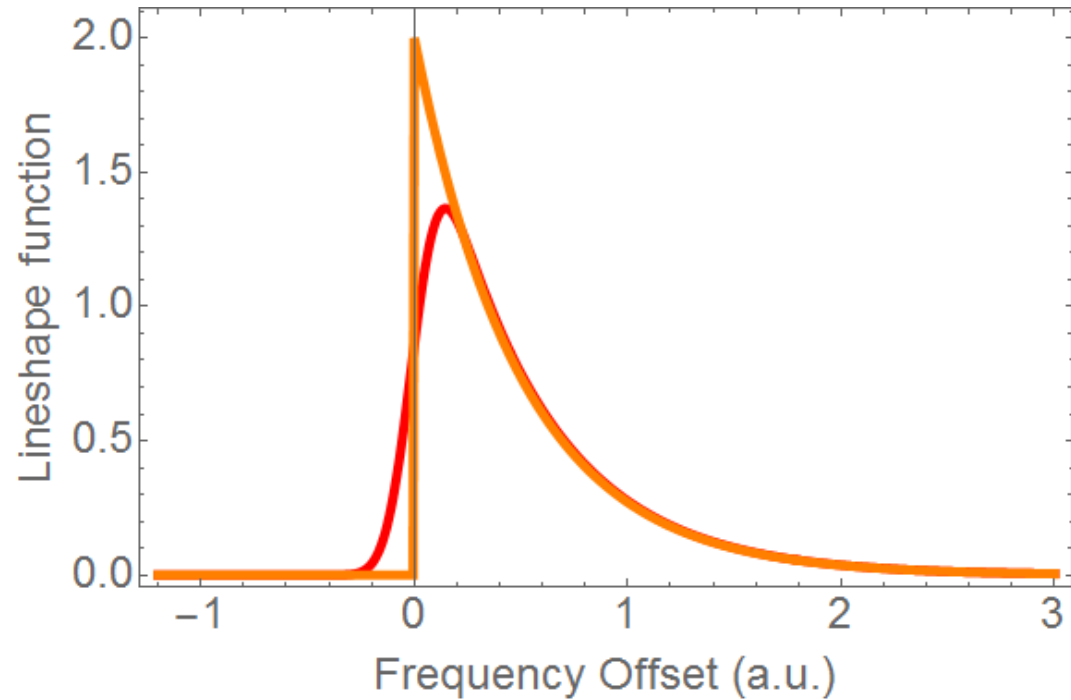


# Measurements in the magnetic bottle



$$\omega_c = \frac{q}{m} B$$

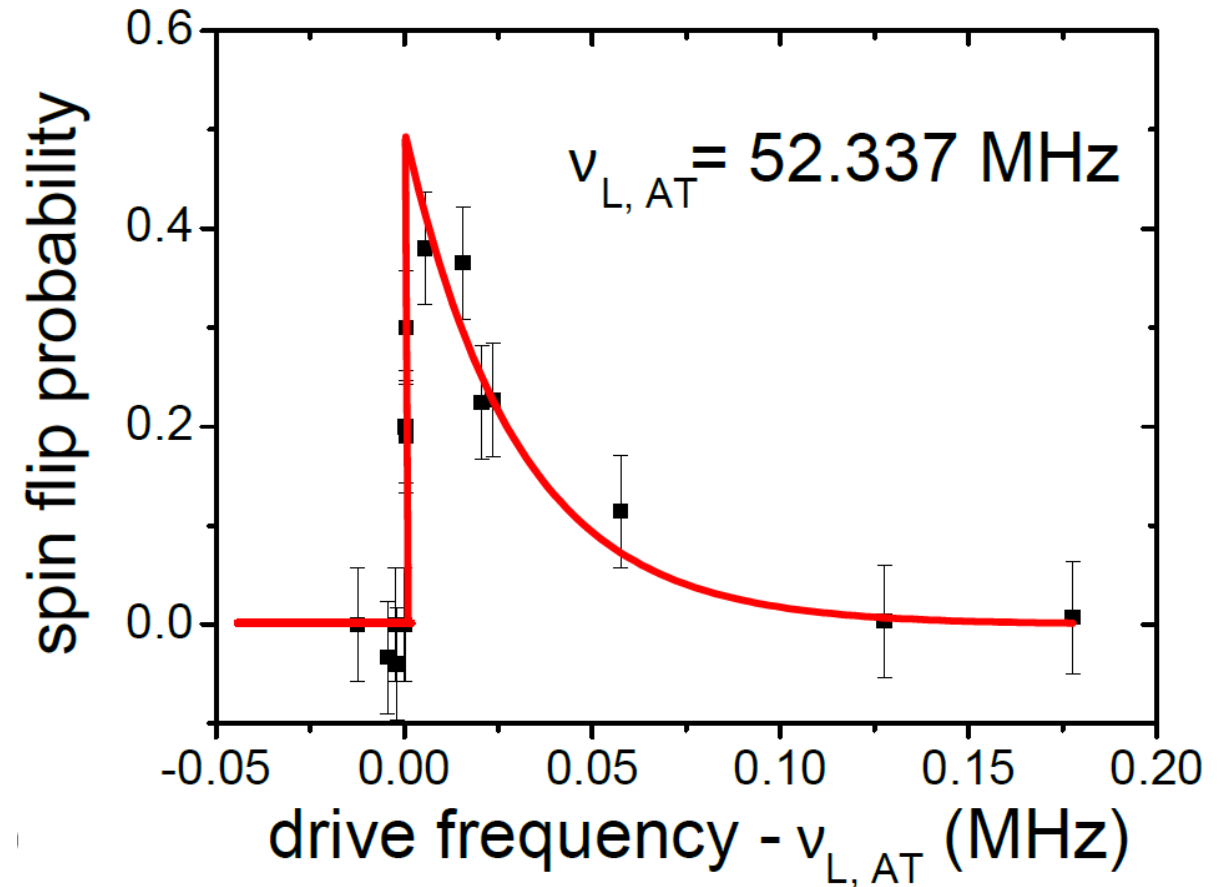
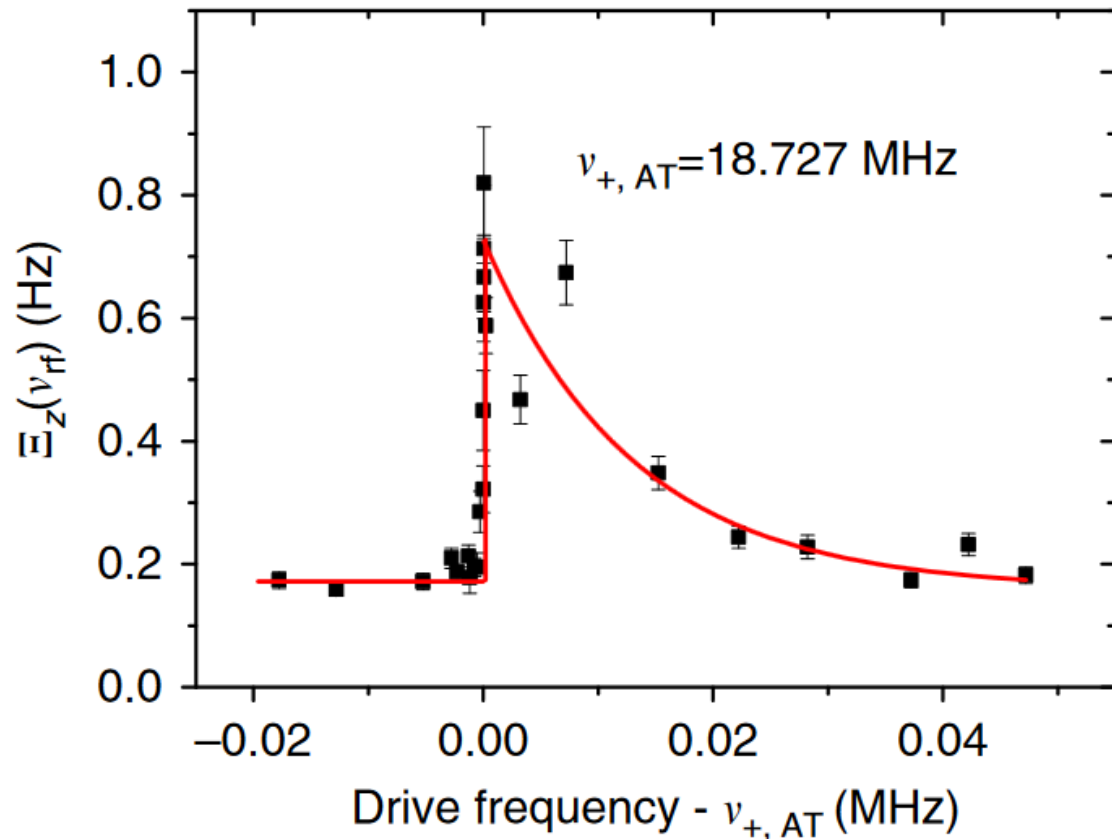
$$\omega_L = g \frac{e}{2m_p} B$$



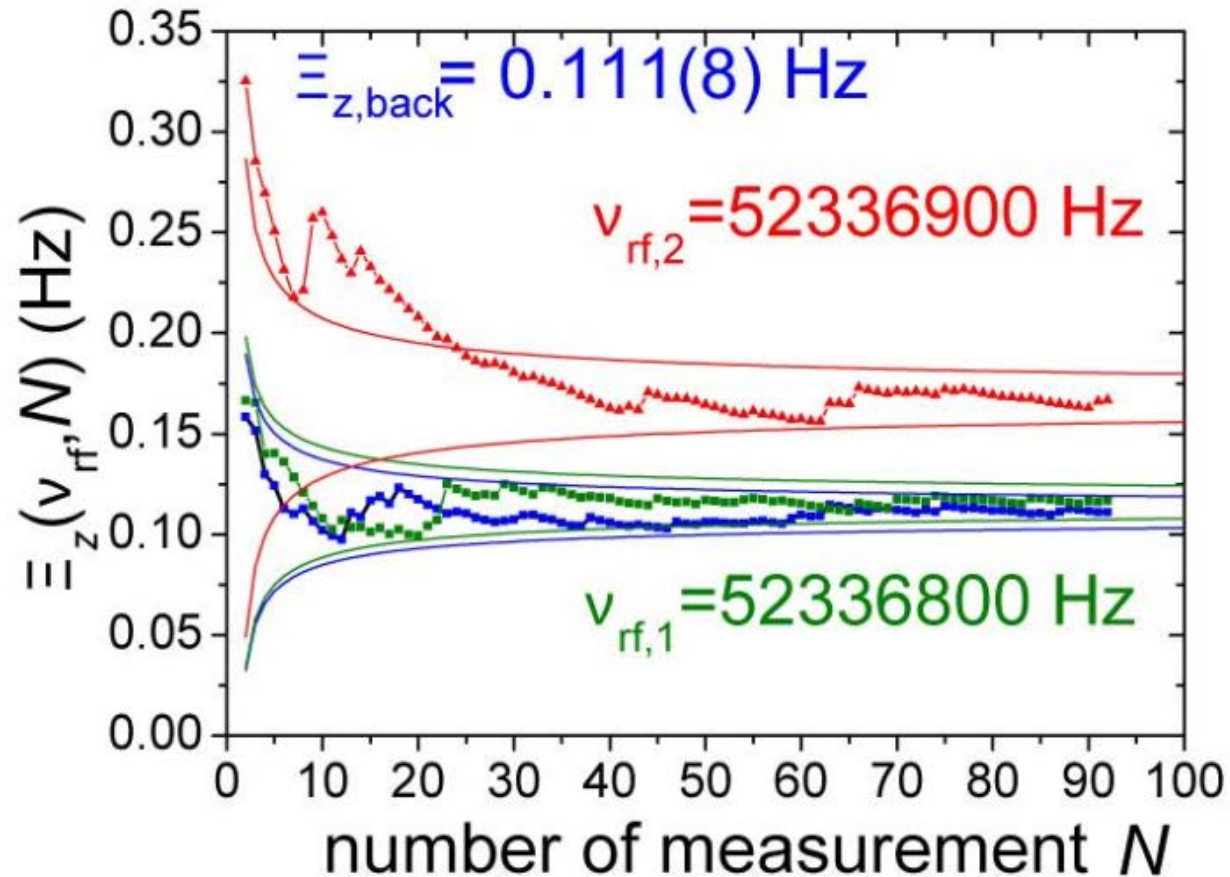
$$\frac{\omega_L}{\omega_c} = \frac{g}{2} = \frac{\mu}{\mu_N}$$

# Alternating measurements of the cyclotron and Larmor cut frequencies

**b**

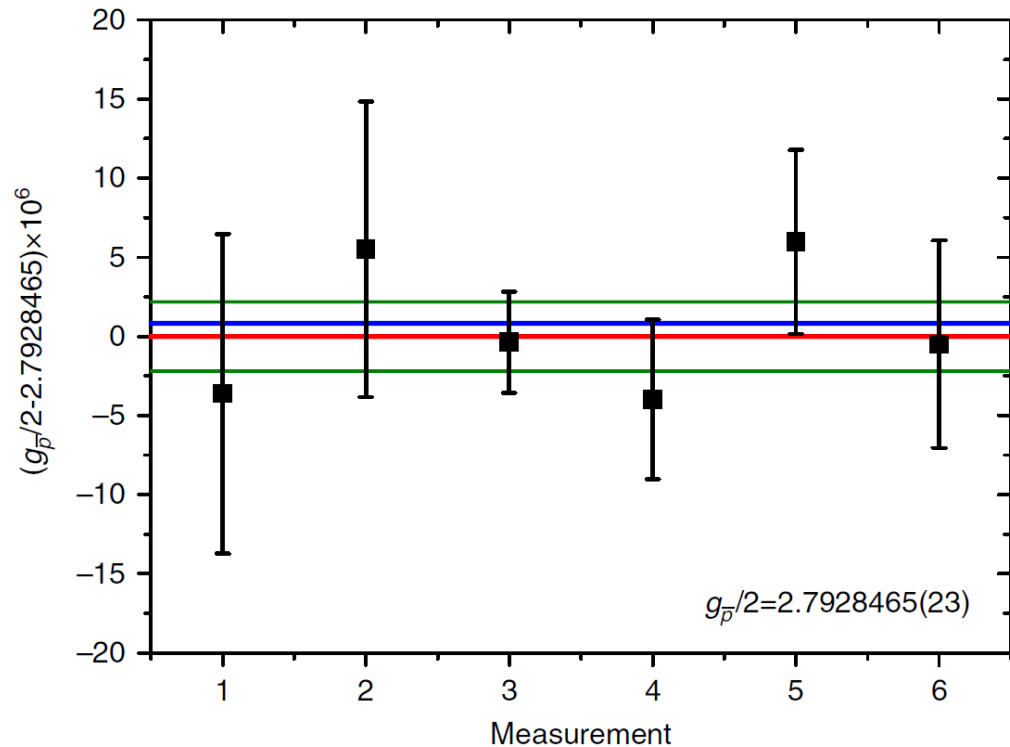


# Larmor frequency cut measurement



$\sim 1$  ppm measurement  
of the Larmor frequency

# Antiproton g-factor results



Six fold improved uncertainty of the antiproton magnetic moment

Respective limits on SME coefficients for CPT violation improved up to a factor 20

**Table 1 | List of all SME-coefficients constrained by this measurement.**

Coefficient	Constraint
$ \tilde{b}_p^Z $	$< 2.1 \times 10^{-22} \text{ GeV}$
$ \tilde{b}_p^{*Z} $	$< 2.6 \times 10^{-22} \text{ GeV}$
$ \tilde{b}_{F,p}^{XX} + \tilde{b}_{F,p}^{YY} $	$< 1.2 \times 10^{-6} \text{ GeV}^{-1}$
$ \tilde{b}_{F,p}^{ZZ} $	$< 8.8 \times 10^{-7} \text{ GeV}^{-1}$
$ \tilde{b}_{F,p}^{*XX} + \tilde{b}_{F,p}^{*YY} $	$< 8.3 \times 10^{-7} \text{ GeV}^{-1}$
$ \tilde{b}_{F,p}^{*ZZ} $	$< 3.0 \times 10^{-6} \text{ GeV}^{-1}$

$$g_{\bar{p}}/2 = 2.7928465(23)$$

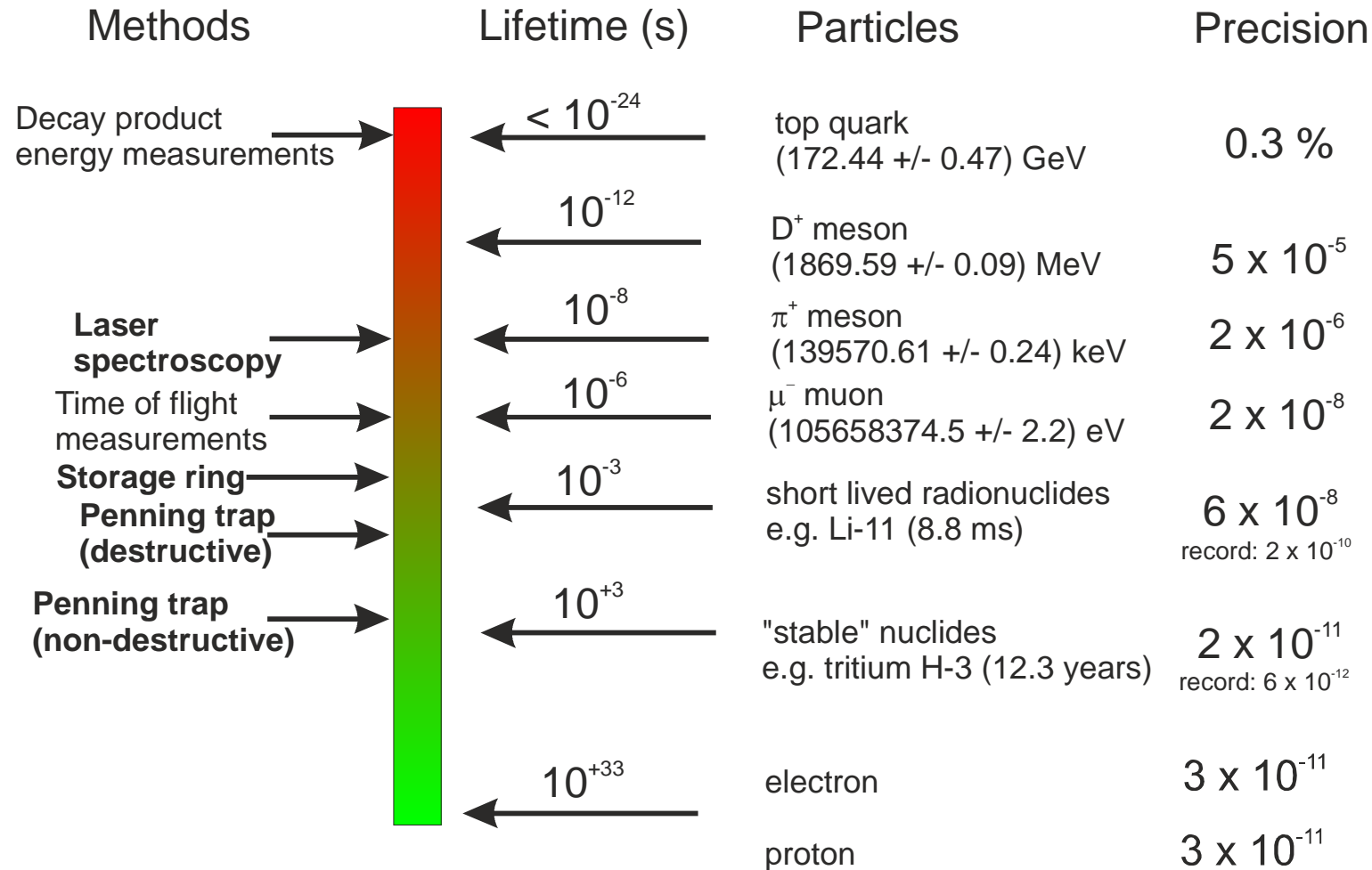
Mass or charge-to-mass ratio  
measurements of fundamental particles



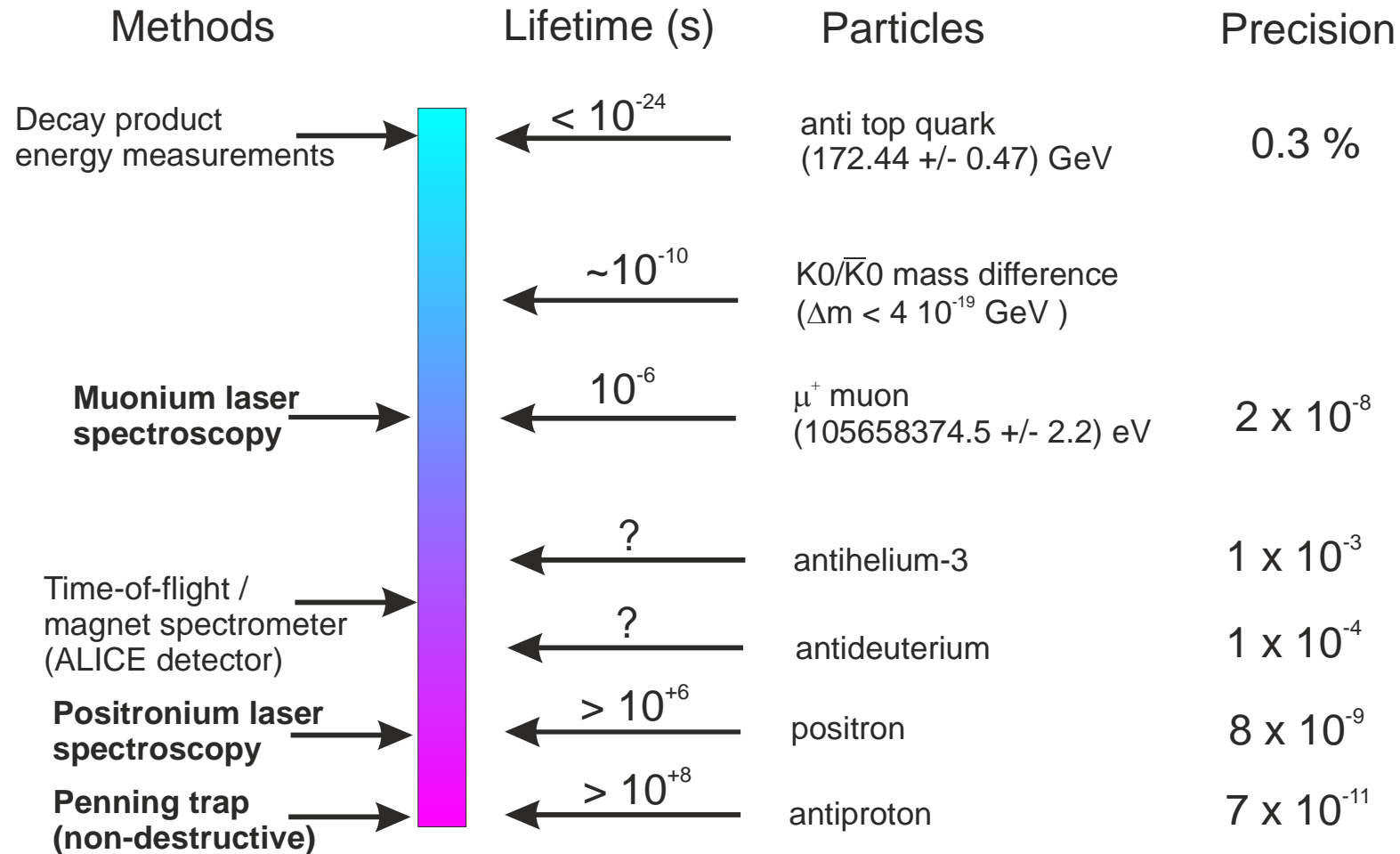
# Applications of Mass Spectrometry

Field	Required relative precision $\delta m/m$
Applied Physics/Chemistry: Identification of atoms/molecules, sample analysis	$10^{-5} - 10^{-6}$
Nuclear Physics/Nuclear Structure	$10^{-6} - 10^{-7}$
Astrophysics: Nucleosynthesis	$10^{-7}$
Weak interaction tests: CVC hypothesis, CKM unitarity	$10^{-8}$
Atomic physics: Binding energies, Neutrino physics: Beta decay Q-values	$10^{-9} - 10^{-11}$
Fundamental Constants, Tests of Quantum Electrodynamics and CPT Symmetries	As high as possible, $< 10^{-10}$

# Lifetime, Methods, and Measurement Precision



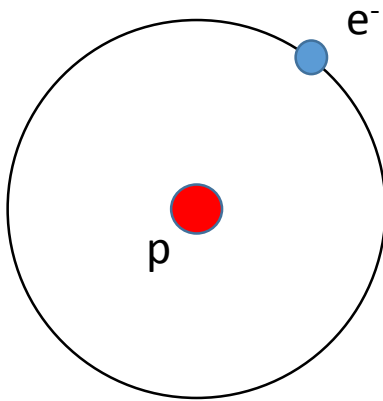
# Anti-Lifetime, Anti-Methods, and Anti-Measurement Precision



# What is an exotic atom?

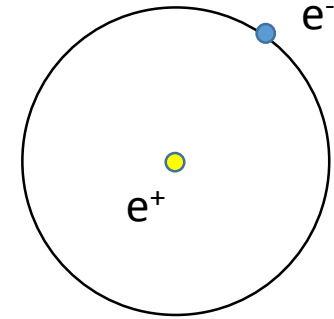
NOT AN EXOTIC ATOM

Hydrogen

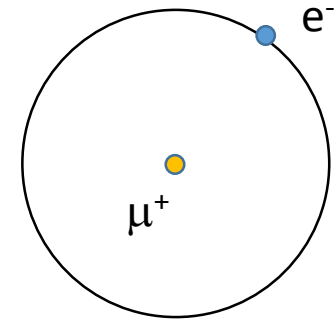


SOME EXAMPLES FOR EXOTIC ATOMS

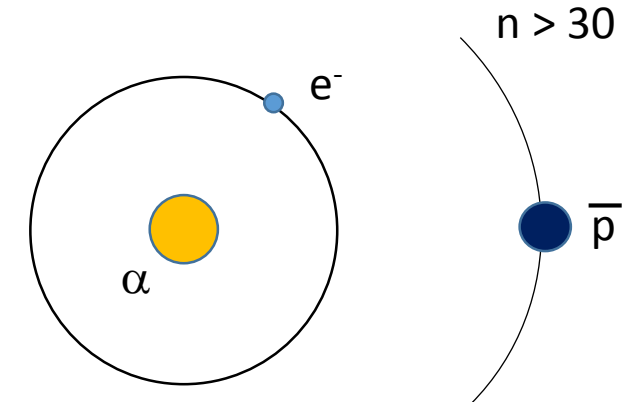
Positronium



Muonium



Antiprotonic Helium



Bohr Atomic Model:

$$E = -Ry h c \frac{Z^2}{n^2} \quad Ry = \frac{e^4}{8 \epsilon_0^2 h^3 c} \frac{m_e m_p}{(m_e + m_p)}$$

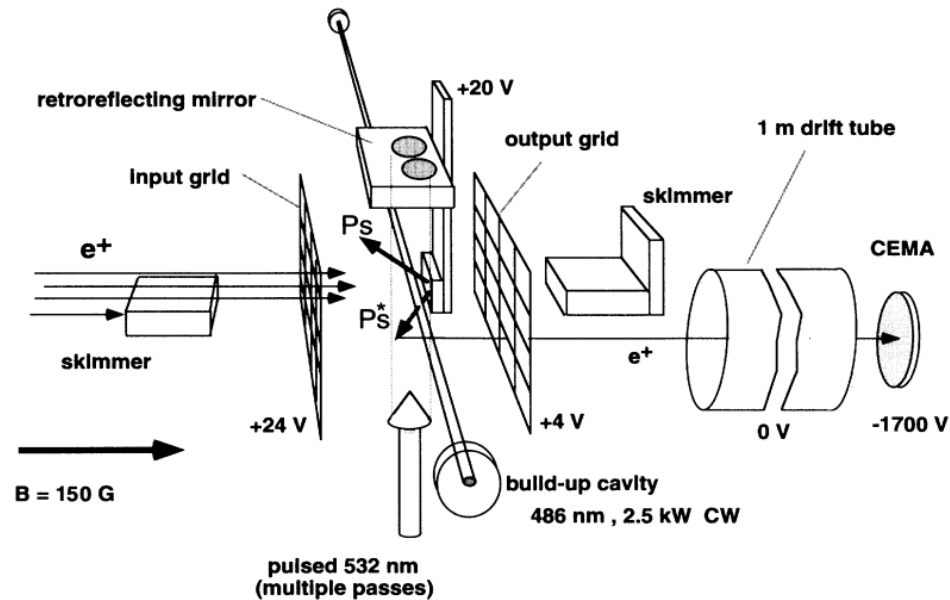
# (Anti)particle masses from transition frequencies

- Spectroscopy of transition frequencies in exotic atoms can constrain the mass ratio of the constituents
- The reduced mass in the Rydberg constant allows to extract the mass ratio of the constituents.
- $Ry_\infty$  known from hydrogen spectroscopy to  $10^{-12}$

$$Ry = Ry_\infty \frac{\mu}{m_e} = Ry_\infty \frac{m_1}{m_e} \frac{1}{\left(\frac{m_1}{m_2} + 1\right)}$$

- Transition frequencies:  $\nu = \frac{E=5eV}{h} \approx 10^{15}$  Hz
- Linewidth due to lifetime of the ground-state:  $\Delta\nu = \frac{1}{2\pi \tau=100 \text{ ns}} \approx 10^6$  Hz
- Promises high precision despite short half-life!
- Transition frequencies include QED corrections (the Lamb shift), which need to be known to the mass-ratio measurement accuracy

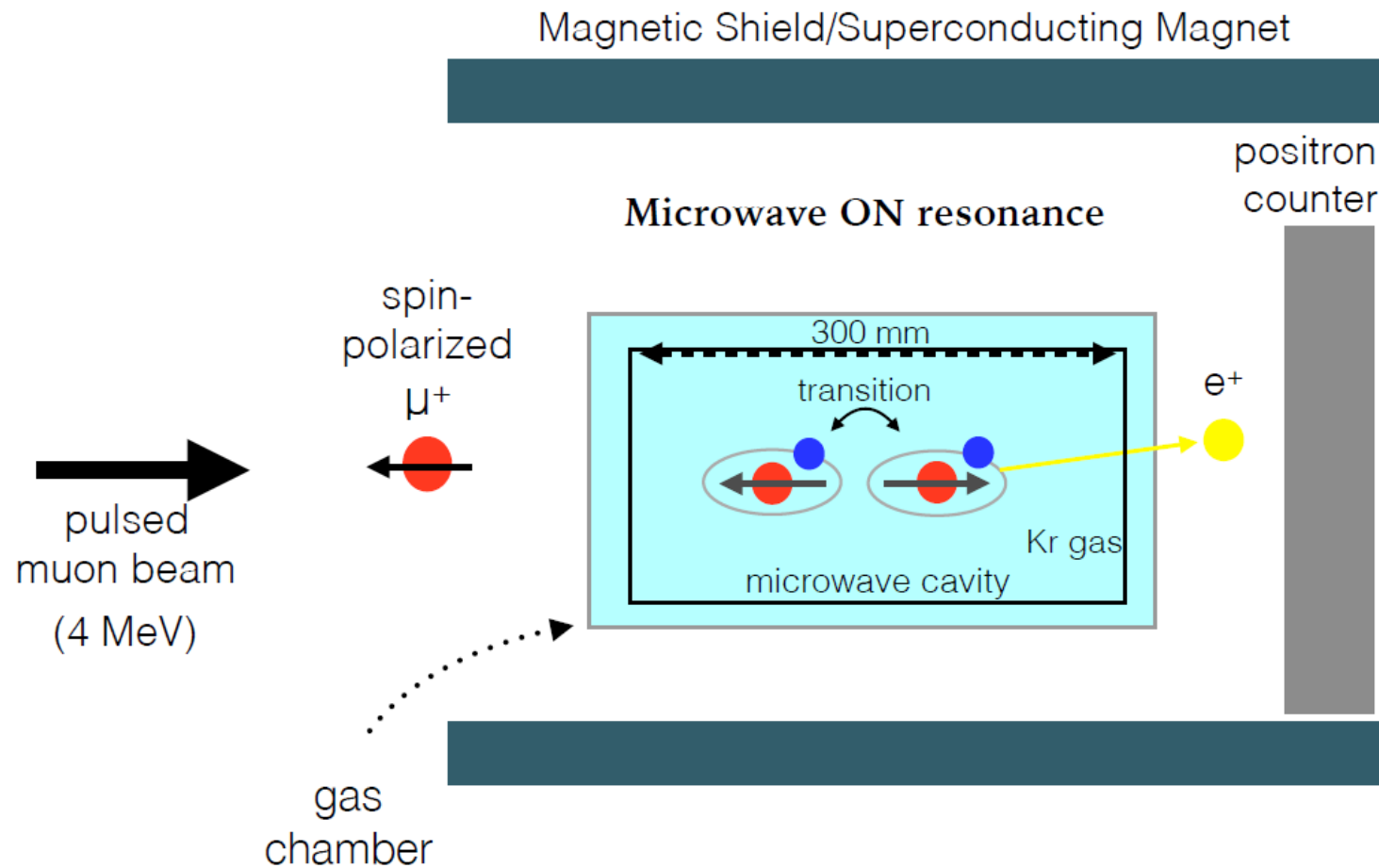
# Example: 1S-2S Positronium spectroscopy



1S-2S transition frequency	$616\,803\,608.2 \pm 1.6$ MHz
1S-2S interval	$1\,233\,607\,216.4 \pm 3.2$
Theory Fell [14]	$1\,233\,607\,221.7 \pm 0(10)$

$$\Rightarrow \frac{|m_{e^+} - m_{e^-}|}{m_{e^-}} < 8 \cdot 10^{-9}$$

# Muonium hyperfine splitting (MuSEUM@J-PARC)

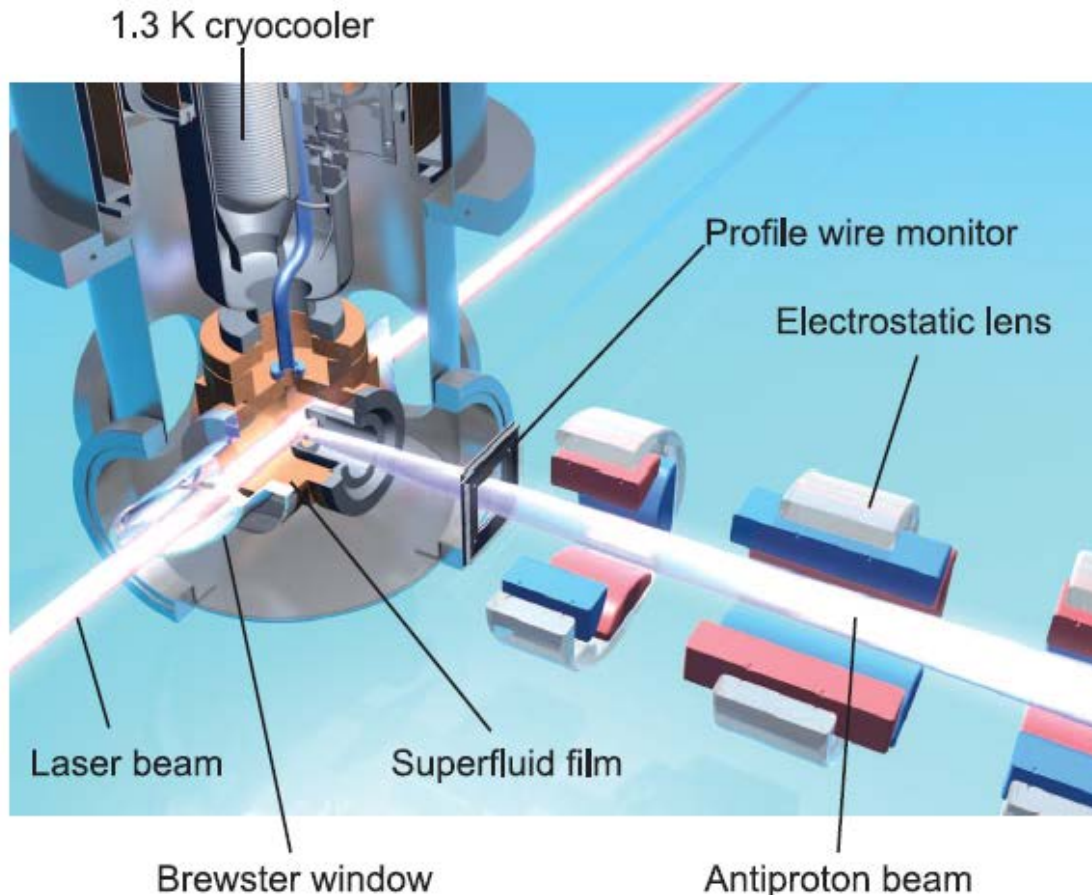


$$\Delta\nu_{HFS} \propto \mu_\mu$$

$$\frac{\mu_e}{\mu_\mu} = \frac{g_e}{g_\mu} \frac{m_\mu}{m_e}$$

$$\nu_{QED} = 4\,463\,302\,720 \text{ (253) (98) (3) Hz } (m_\mu/m_e) \text{ (QED) } (\alpha)$$

# Antiprotonic helium experiment (ASACUSA)



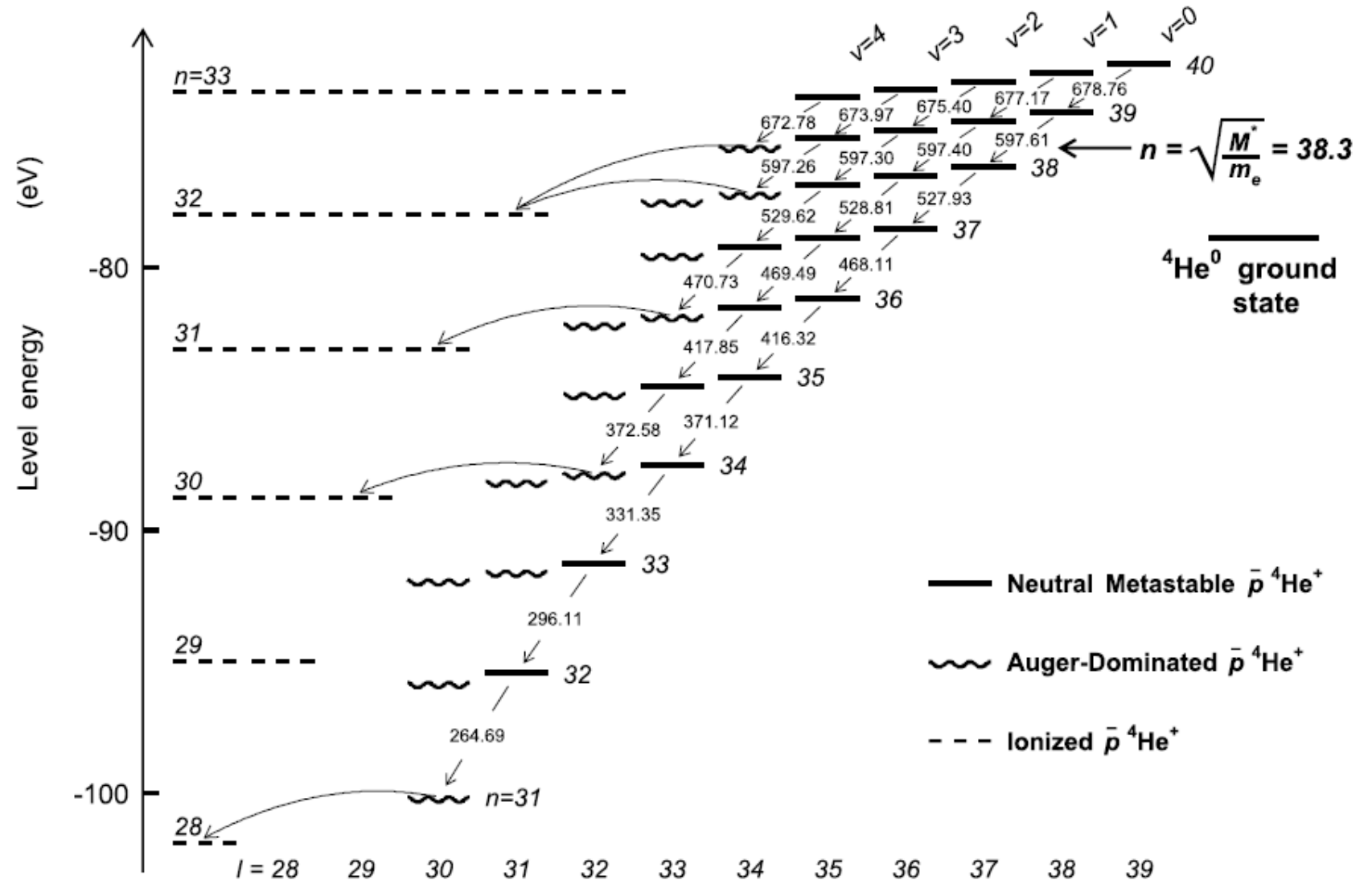
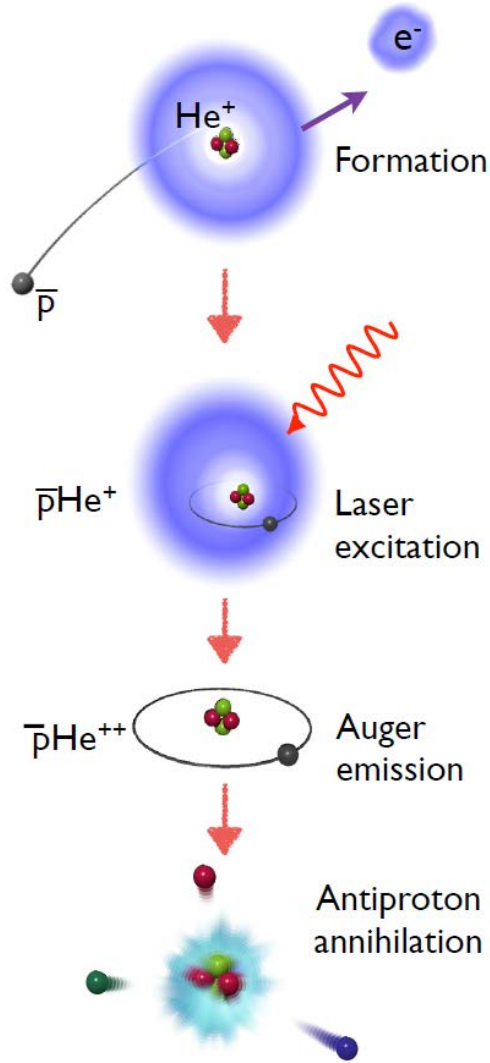
Antiprotons are stopped in thin cold helium gas.

Antiprotonic helium is formed by replacing one of the electrons in the helium atom

Buffer-gas cooling cools the antiprotonic helium atom to low temperatures ( $T \sim 1.6$  K)

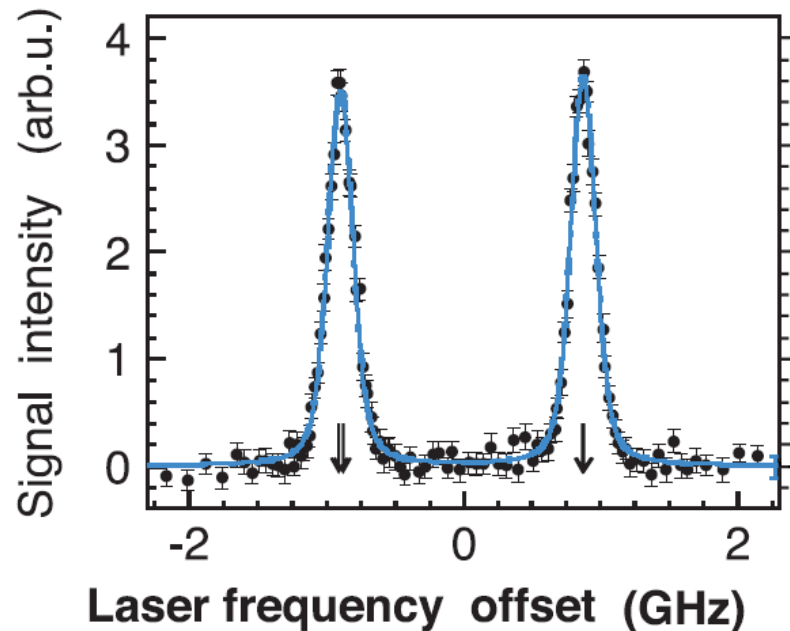


# Antiprotonic Helium



# Antiproton-to-electron mass ratio

Example signal



Single photon spectroscopy of antiprotonic helium at 1.6 (0.1) K

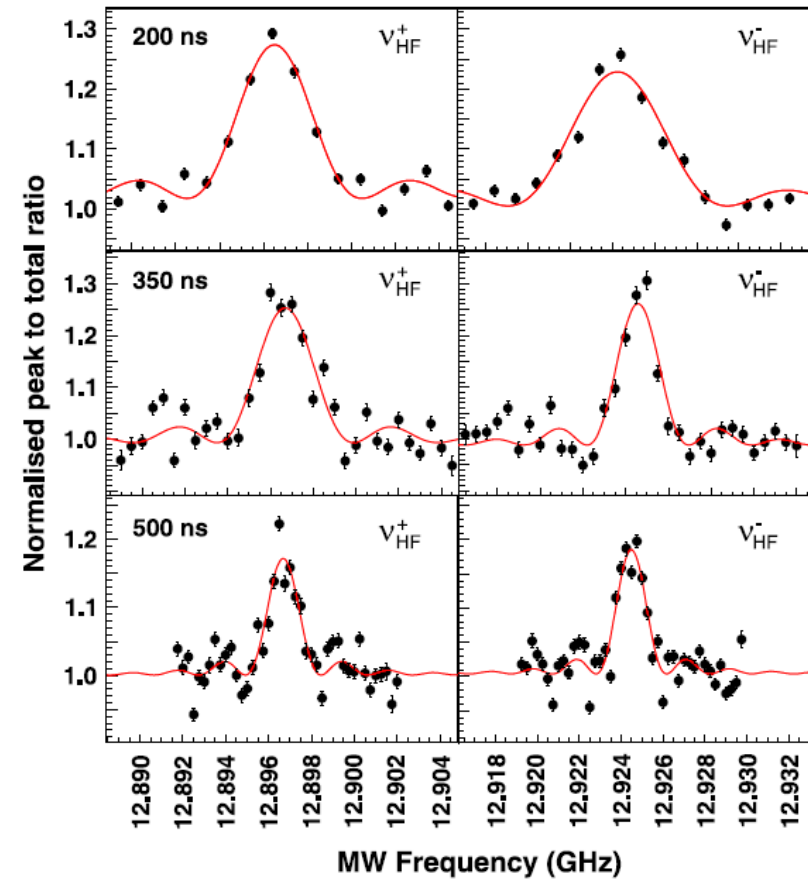
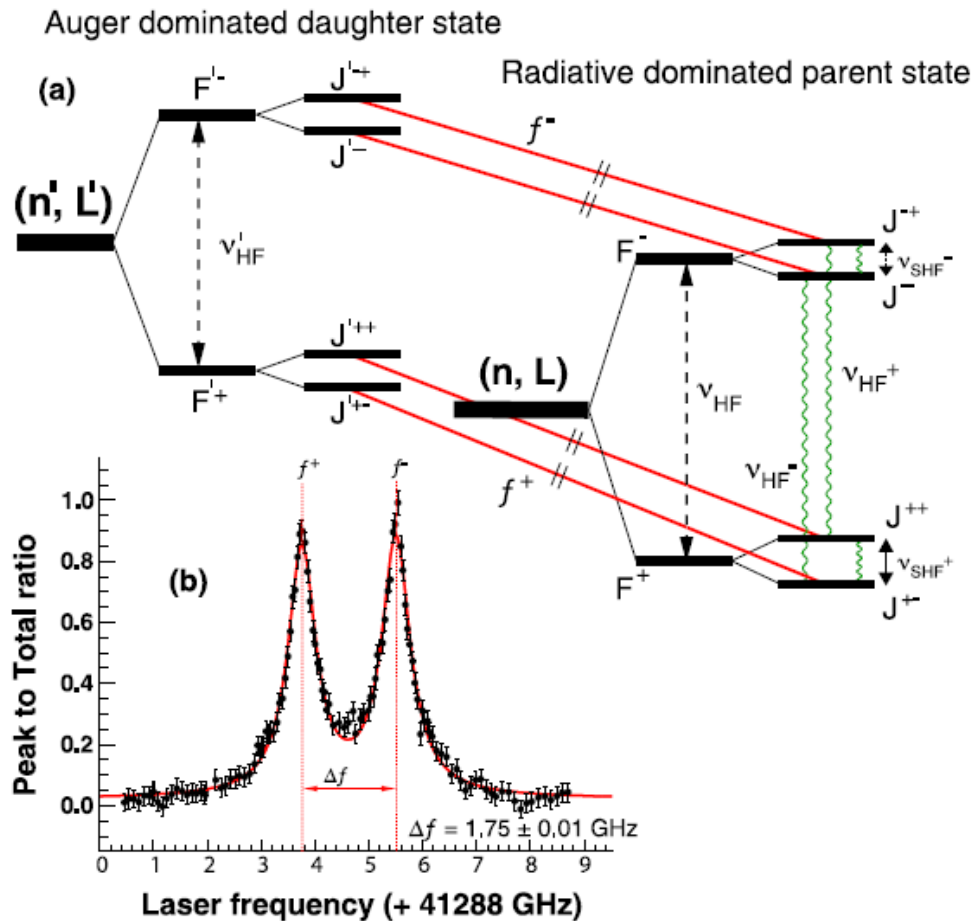
Comparison of experiment and QED calculations allows to extract the antiproton-to-electron mass ratio

$$h\nu_{th} \approx \frac{m_{\bar{p}}}{m_e} Z_{eff}^2 R_y \left( \frac{1}{n'^2} - \frac{1}{n^2} \right)$$

Recent measurements improve this value to  $8 \cdot 10^{-10}$  relative uncertainty

Result is in agreement with CPT invariance

# Antiproton magnetic moment from the “super fine structure”

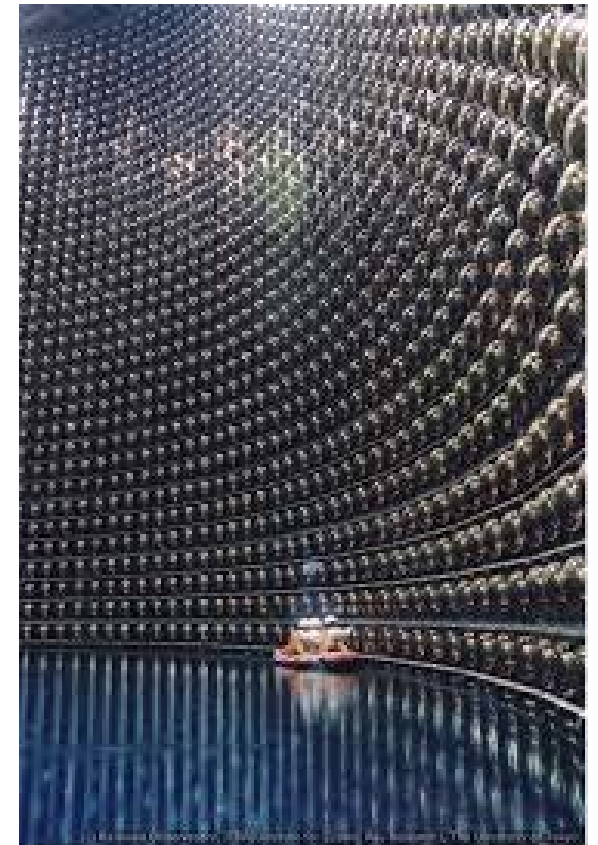


$$\mu_S^{\bar{p}} = -2.7862(83) \mu_N$$

Antiproton lifetime limits

# Motivation

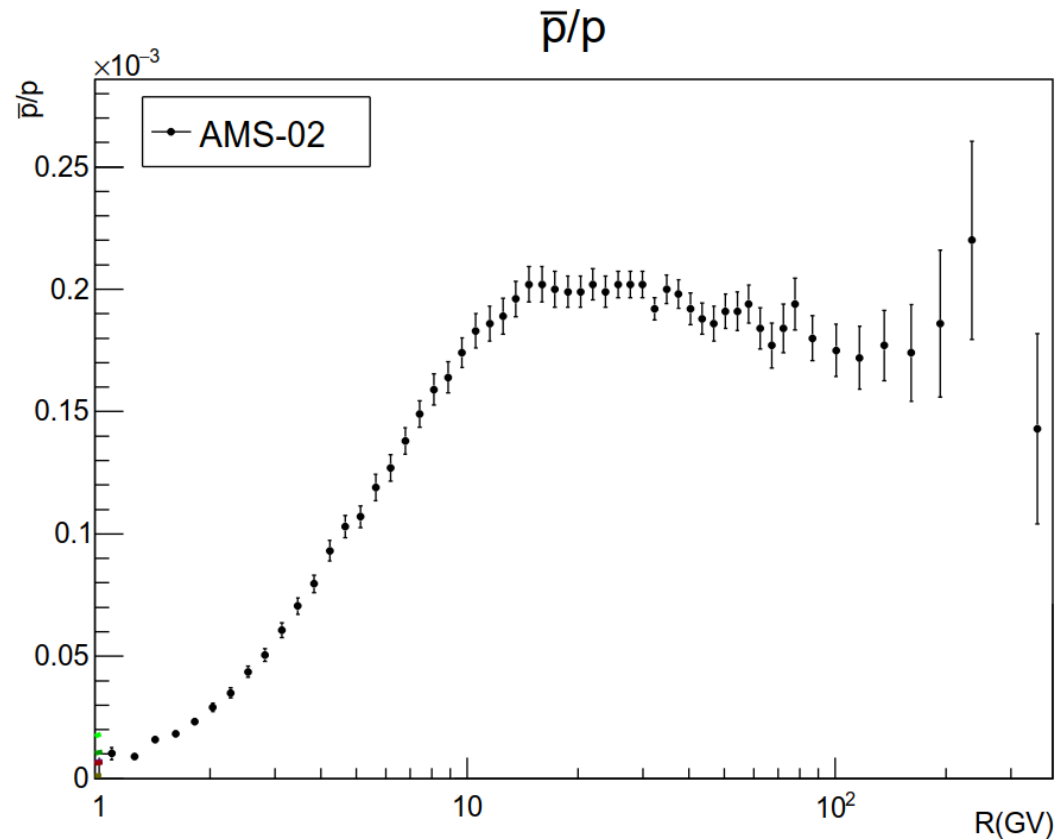
- A proton and antiproton lifetime comparison tests
  - CPT invariance
  - B-violation
- Super-Kamiokande experiment
  - Proton lifetime: invisible modes  $\tau > 10^{29}$  y  
specific channels  $1/\Gamma_i > 10^{34}$  y
  - Sample: 50000 tons of purified water



Superkamiokande Experiment

# Antiproton lifetime limits from cosmology

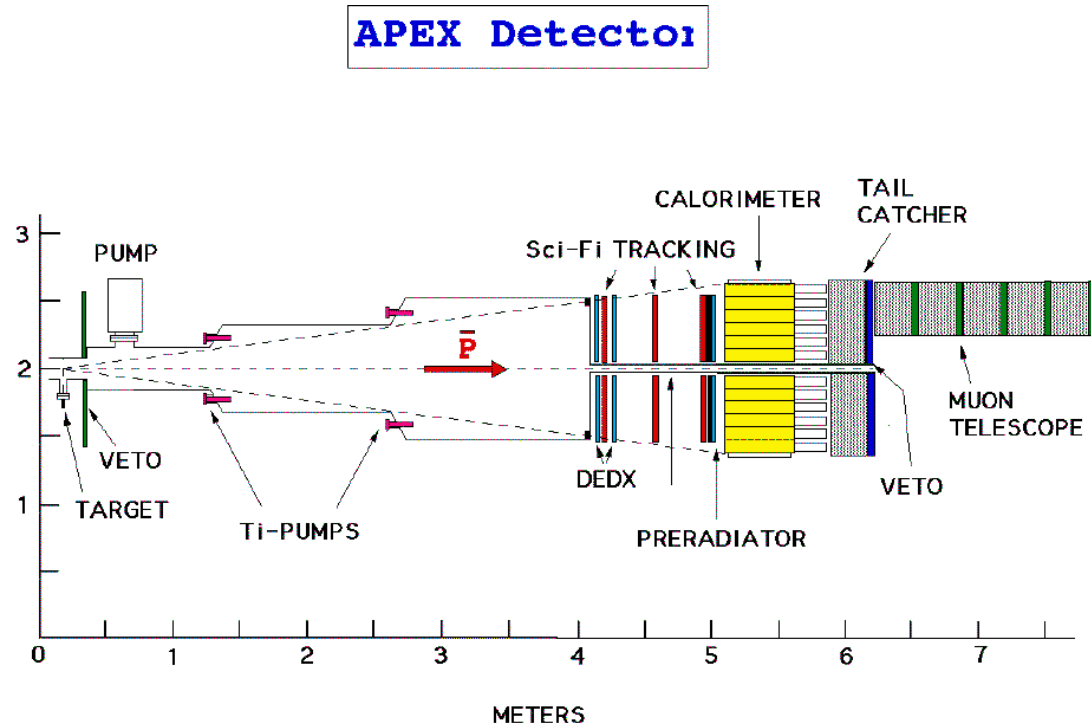
Cosmic ray flux analysed with the Alpha Magnetic Spectrometer (ISS)



- How long do these antiprotons exist until they reach us?
- How many antiprotons do we expect to see?
- Limit depends on model dependent parameters on antiproton production, propagation and interaction in the interstellar medium
- $\tau_{\bar{p}} > 8 \cdot 10^5 \text{ y}$

# APEX Experiment at Fermilab (~1999)

Search for antiproton decay product from antiprotons cycling in a storage ring



# APEX results

TABLE I. Summary of results: 90% C.L. limits on  $\tau/B$  for 15 antiproton decay modes.

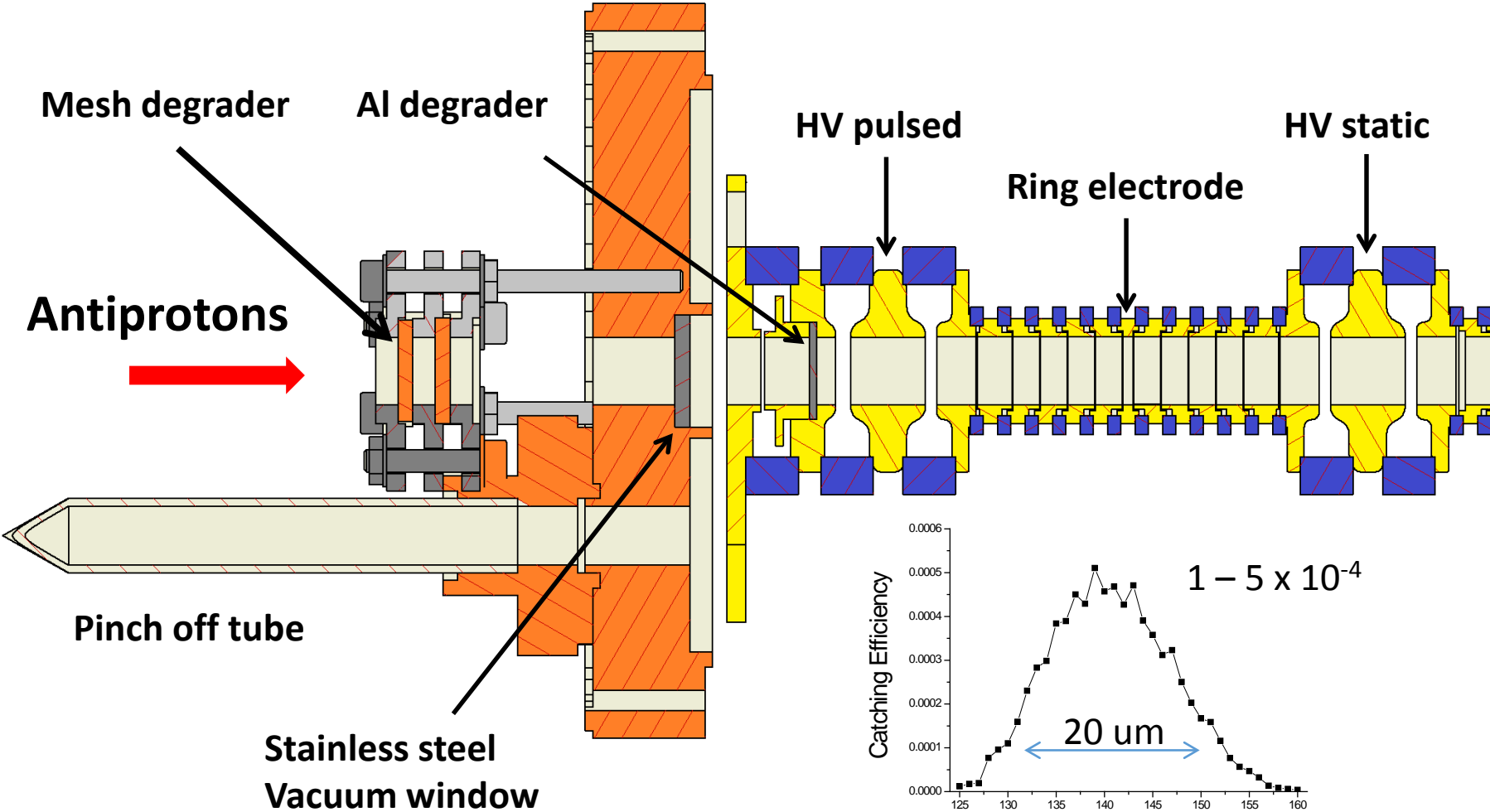
Decay mode	$\tau/B$ Limit (years)	Decay mode	$\tau/B$ Limit (years)
$\mu^- \gamma$	$5 \times 10^4$	$e^- \gamma$	$7 \times 10^5$
$\mu^- \pi^0$	$5 \times 10^4$	$e^- \pi^0$	$4 \times 10^5$
$\mu^- \eta$	$8 \times 10^3$	$e^- \eta$	$2 \times 10^4$
$\mu^- \gamma\gamma$	$2 \times 10^4$	$e^- \gamma\gamma$	$2 \times 10^4$
$\mu^- K_L^0$	$7 \times 10^3$	$e^- K_L^0$	$9 \times 10^3$
$\mu^- K_S^0$	$4 \times 10^3$	$e^- K_S^0$	$9 \times 10^2$
		$e^- \rho$	$2 \times 10^2$
		$e^- \omega$	$2 \times 10^2$
		$e^- K^{0*}$	$1 \times 10^3$



# Deceleration from 5.3 MeV to 0.5 meV

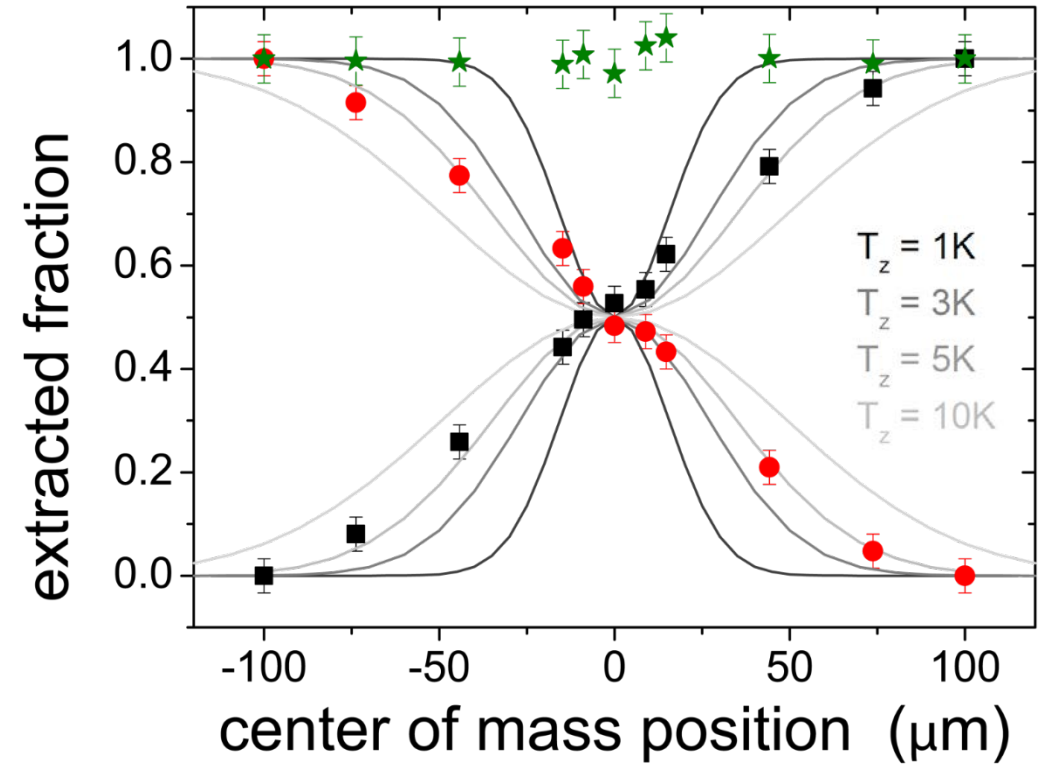
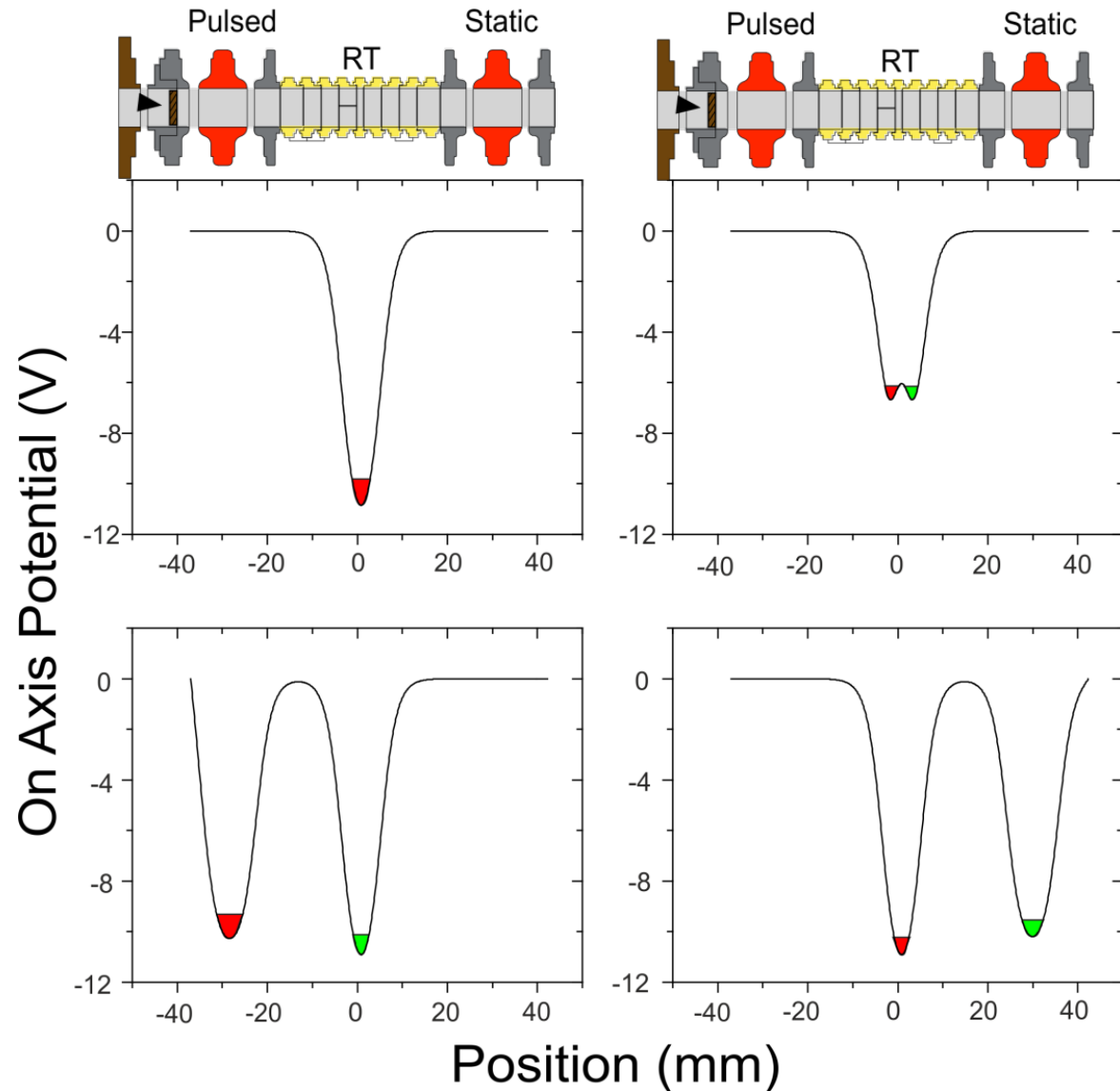
Isolation vacuum:  $\sim 10^{-8}$  mbar

Trap can vacuum:  $< 10^{-18}$  mbar



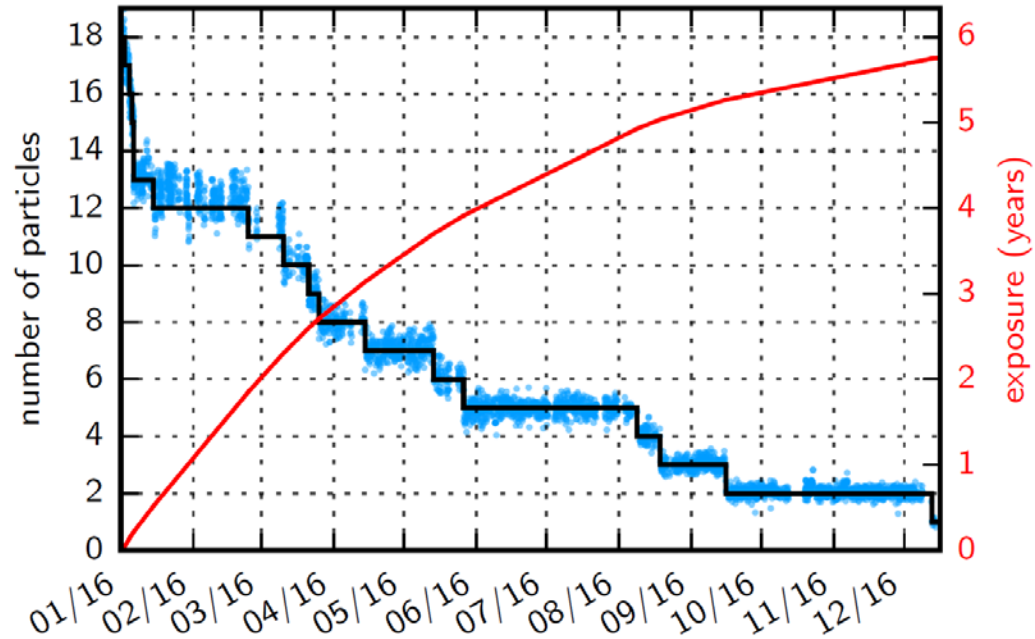
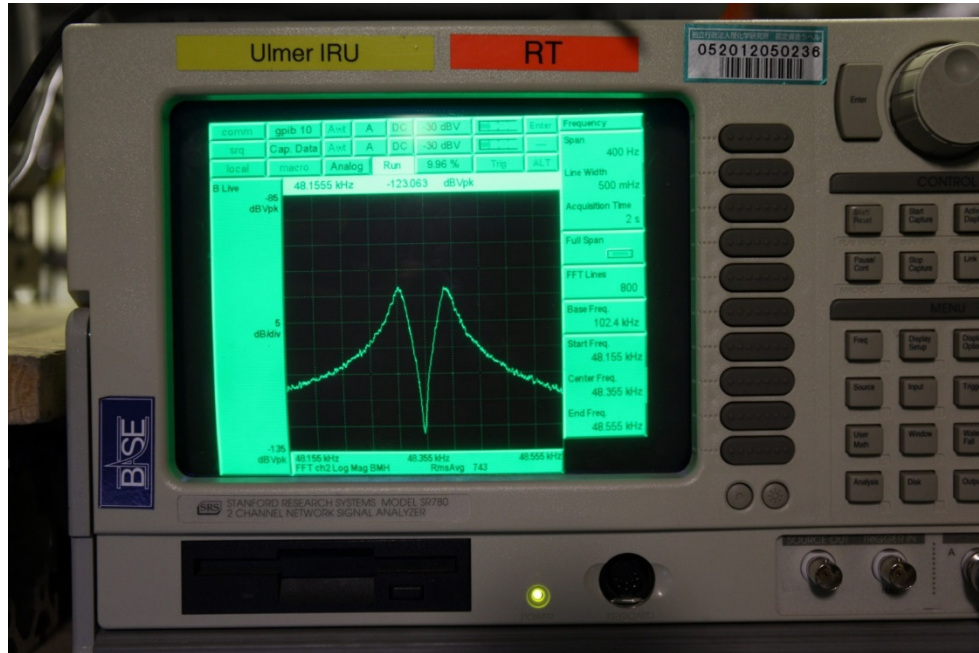
C. Smorra et al., Int. J. Mass Spectr. **389**, 10 (2015).  
 S. Sellner et al., New J. Phys. **19**, 083023 (2017).

# Non-destructive extraction: Separate and Merge



# Reservoir trap

Antiprotons stored from 03.11.2015 – 22.12.2016



- Storage of antiprotons for more than one year: **405.5 days**
- Extraction of single particles by a potential tweezer scheme

C. Smorra et al., Int. J. Mass Spectr. **389**, 10 (2015).  
S. Sellner et al., New J. Phys. **19**, 083023 (2017).

Inversion of the baryon asymmetry:

Antibaryon density:  $\sim 10^8/\text{cm}^3$

$V < (50 \mu\text{m})^3$

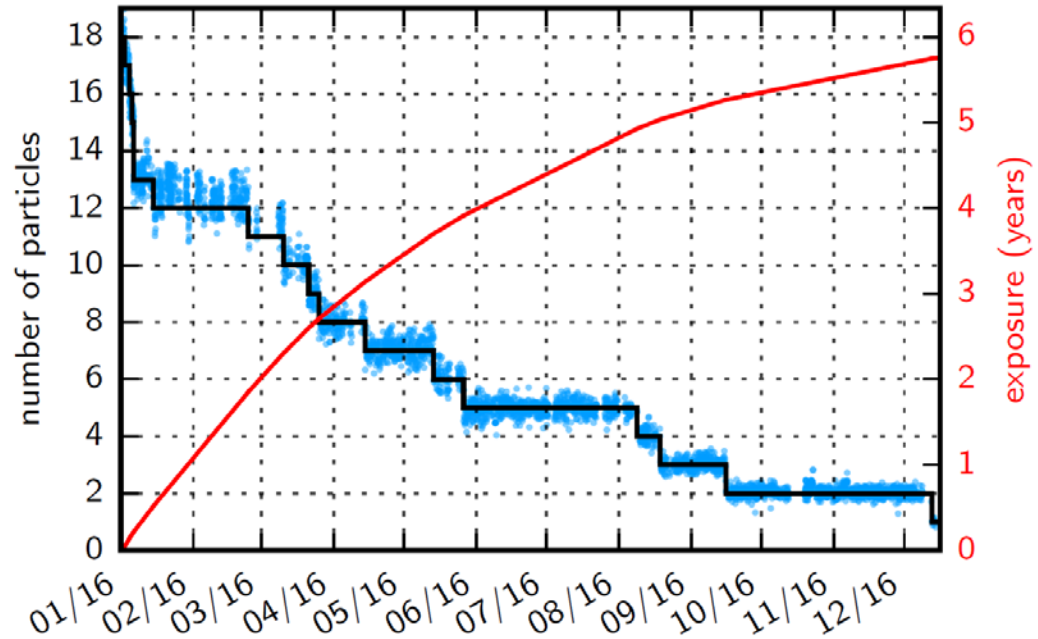
Baryon density:  $\sim 1 / \text{cm}^3$

$p < 10^{-16} \text{ Pa}$

# Antiproton Lifetime Limits

**Table 1.** List of individual data sets which contribute to the derived antiproton lifetime limit.

Specific dataset	Exposure time (years)
RT	5.77
Precision traps	1.72
RT systematics	2.61
2014 run	1.56
Sum	11.66



Antiproton lifetime limits:

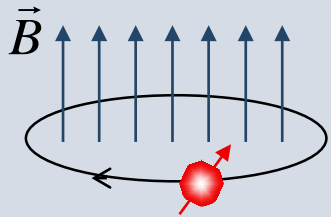
$$\tau_{\bar{p}} > 10.2 \text{ y (68\% C.L.)}$$

$$\tau_{\bar{p}} > 5.0 \text{ y (90\% C.L.)}$$

Penning trap mass spectrometers

# Charge-to-mass ratio determination in Penning traps

## Cyclotron Frequency Ratio



$$\omega_c = \frac{q}{m} B$$

$$\frac{\omega_{c,\bar{p}}}{\omega_{c,p}} = \frac{q_{\bar{p}}/m_{\bar{p}}}{q_p/m_p}$$

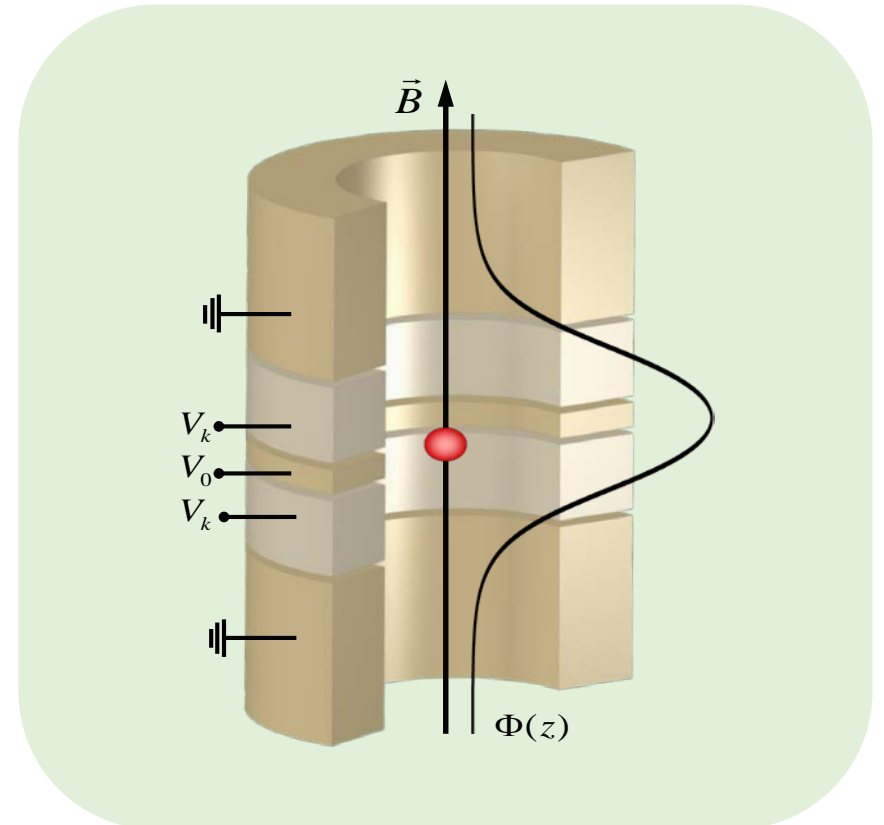
Stable magnetic field:

Superconducting magnet in persistent mode

$$\frac{\delta B}{B} < 10^{-8} / \text{h}$$

Long observation time for precise frequency measurements

Well-controlled contamination-free environment for single particles



H. G. Dehmelt and P. Ekström, Bull. Am. Phys. Soc. 18, 72 (1973).

D. J. Wineland and H. G. Dehmelt, J. Appl. Phys. 46, 919 (1975).

# Basic principles of Penning traps

Radial confinement by a strong homogeneous magnetic field  $B$  ( $\sim 7$  T)

Axial confinement by a weak quadrupolar electric field  $U$  ( $\sim 10$  V) :

$$V(\rho, z) = \frac{U}{2d^2} \left( z^2 - \frac{\rho^2}{2} \right)$$

Motion in the trap:

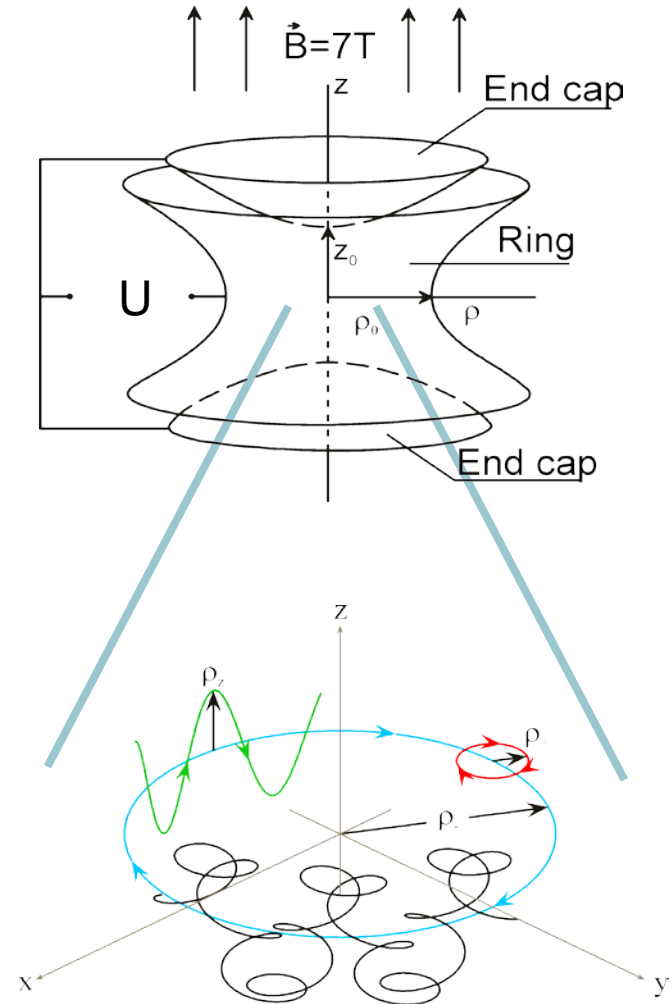
Three independent harmonic oscillators

Axial motion:

$$\omega_z = \sqrt{\frac{q \cdot U}{m \cdot d^2}}$$

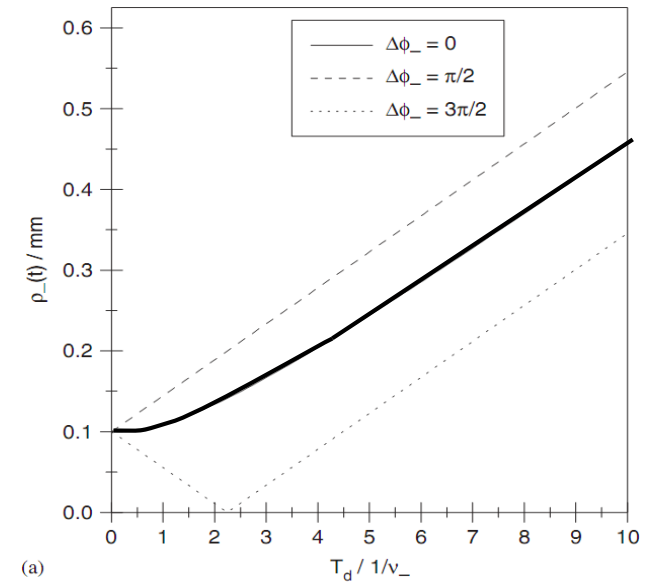
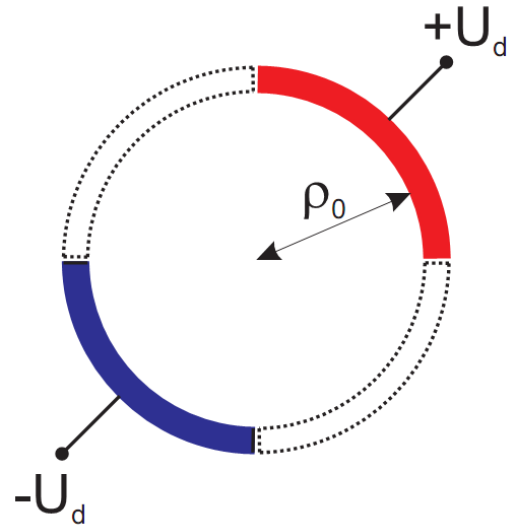
Reduced cyclotron and magnetron motion:

$$\omega_{\pm} = \frac{1}{2} \left( \omega_c \pm \sqrt{\omega_c^2 - 2\omega_z^2} \right)$$



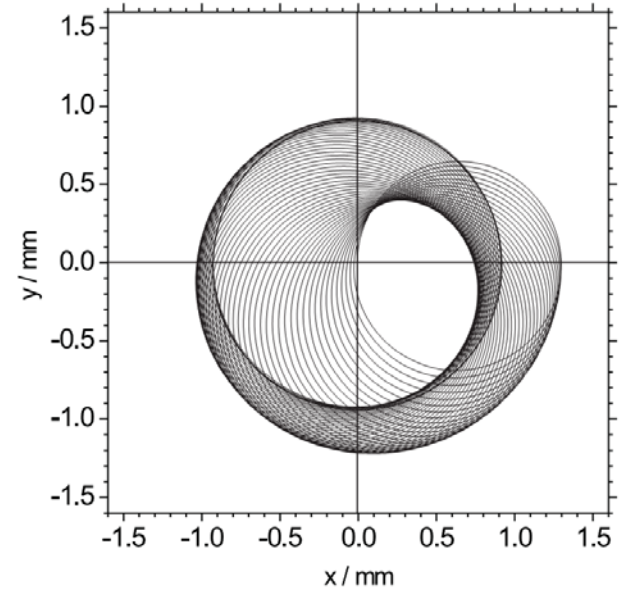
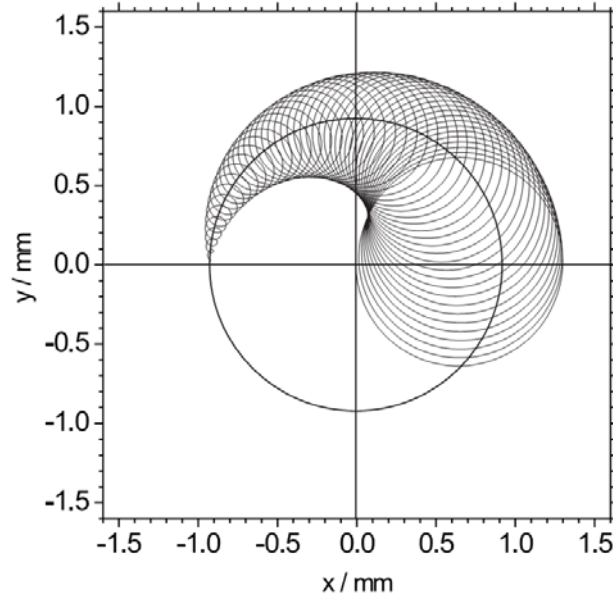
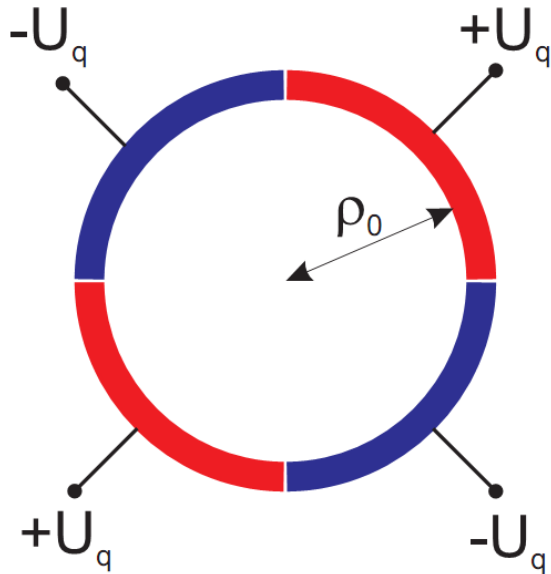
# Ion manipulation in a Penning trap

Dipolar excitation:





# Mode coupling: Quadrupolar excitation

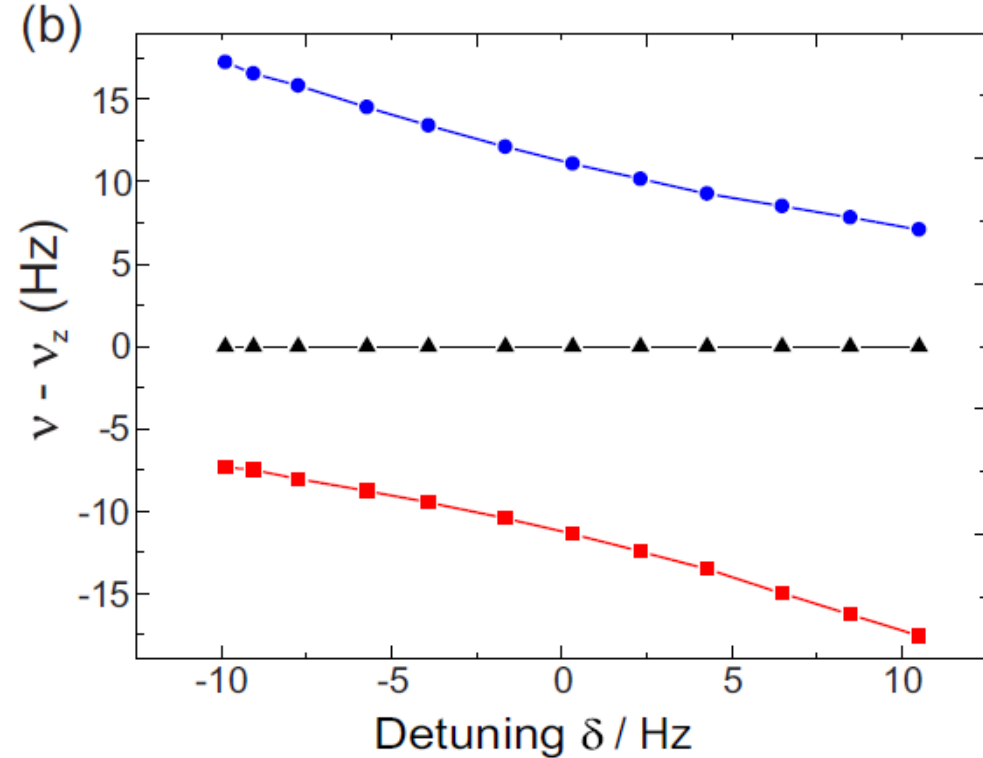
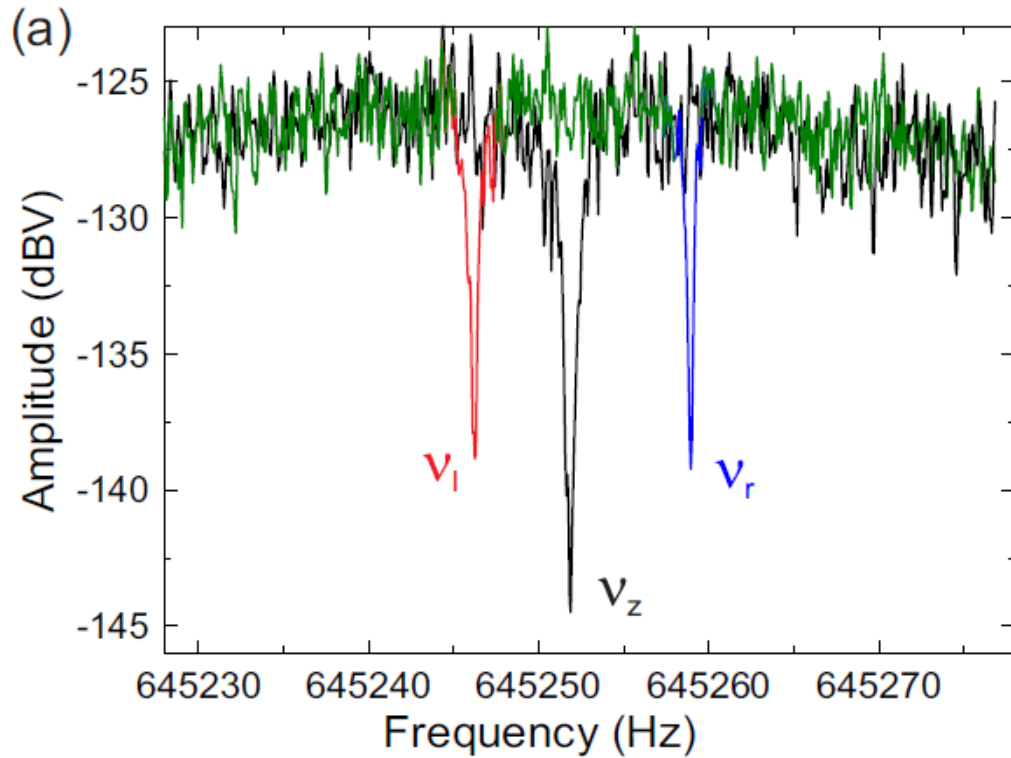


Conversion between two eigenmotions by excitation at the sum frequency:

$$\omega_{rf} = \omega_+ + \omega_-$$

Continuous excitation leads to an amplitude modulation in the two involved trap modes with exchange frequency  $\Omega/2$ .

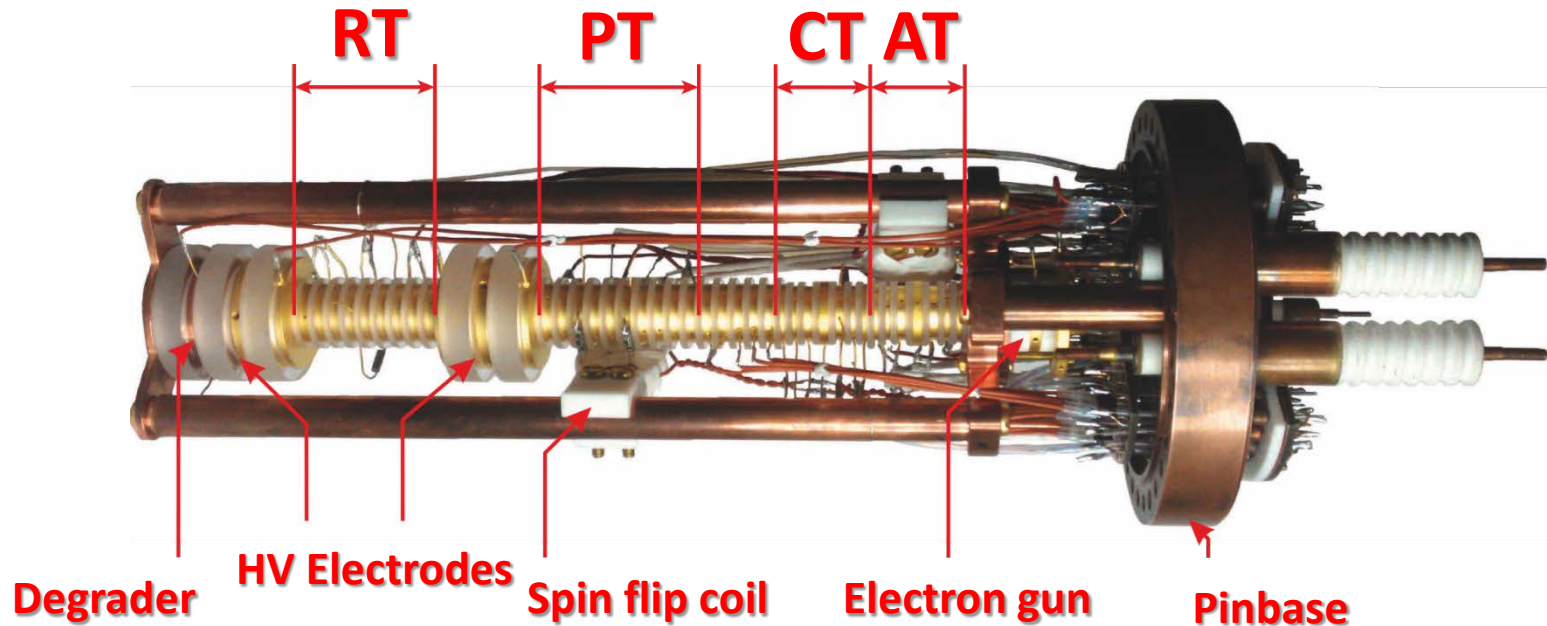
# Axial-cyclotron sideband coupling



$$\nu_{l,r} = \nu_z - \frac{\delta}{2} \pm \sqrt{\frac{\Omega_0^2}{4\pi^2} + \delta^2}$$

$$\nu_+ = \nu_{rf} + \nu_l + \nu_r - \nu_z$$

# The BASE four Penning-trap system



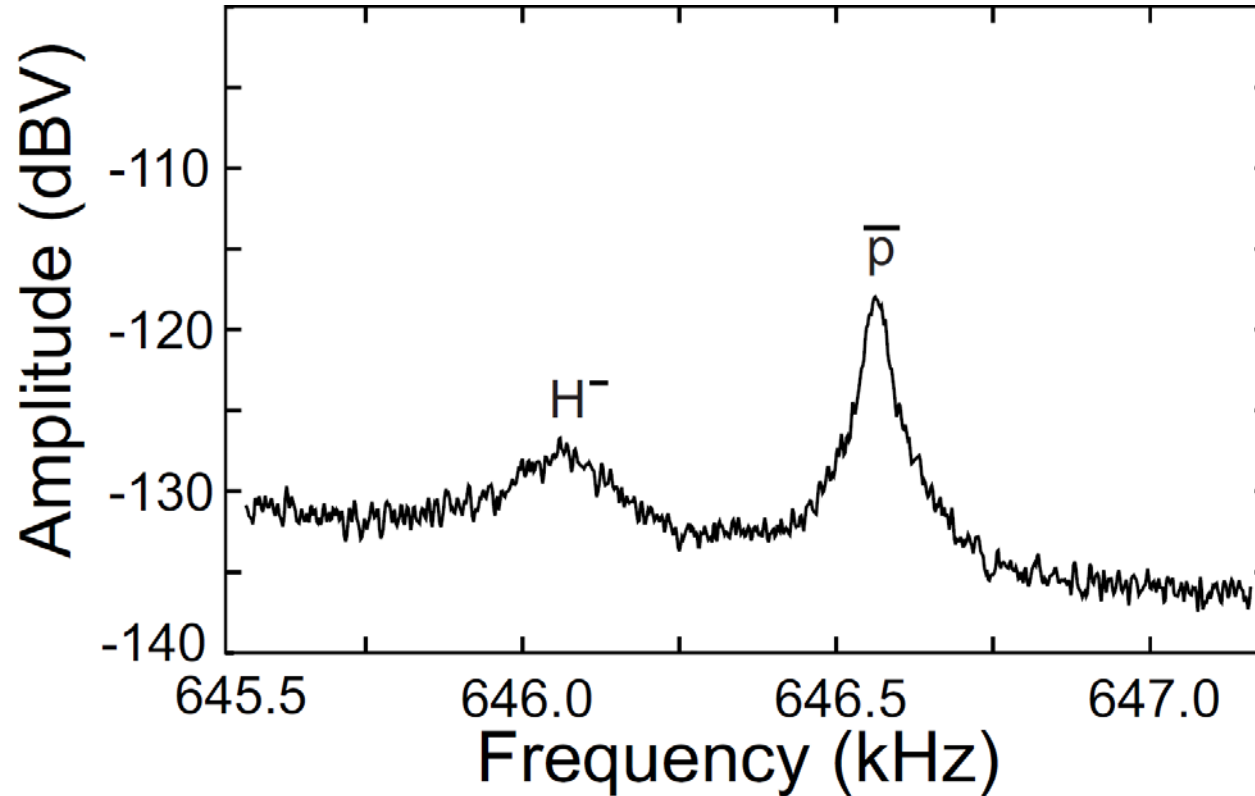
**RT: Catching / Reservoir Trap:** Catching, cooling and storing of antiprotons

**PT: Precision Trap:** Homogeneous magnetic field for precision frequency measurements

**CT: Cooling Trap:** Fast cooling of the cyclotron motion

**AT: Analysis Trap:** Inhomogeneous field for the detection of antiproton spin flips,  $B_2 = 30 \text{ T} / \text{cm}^2$

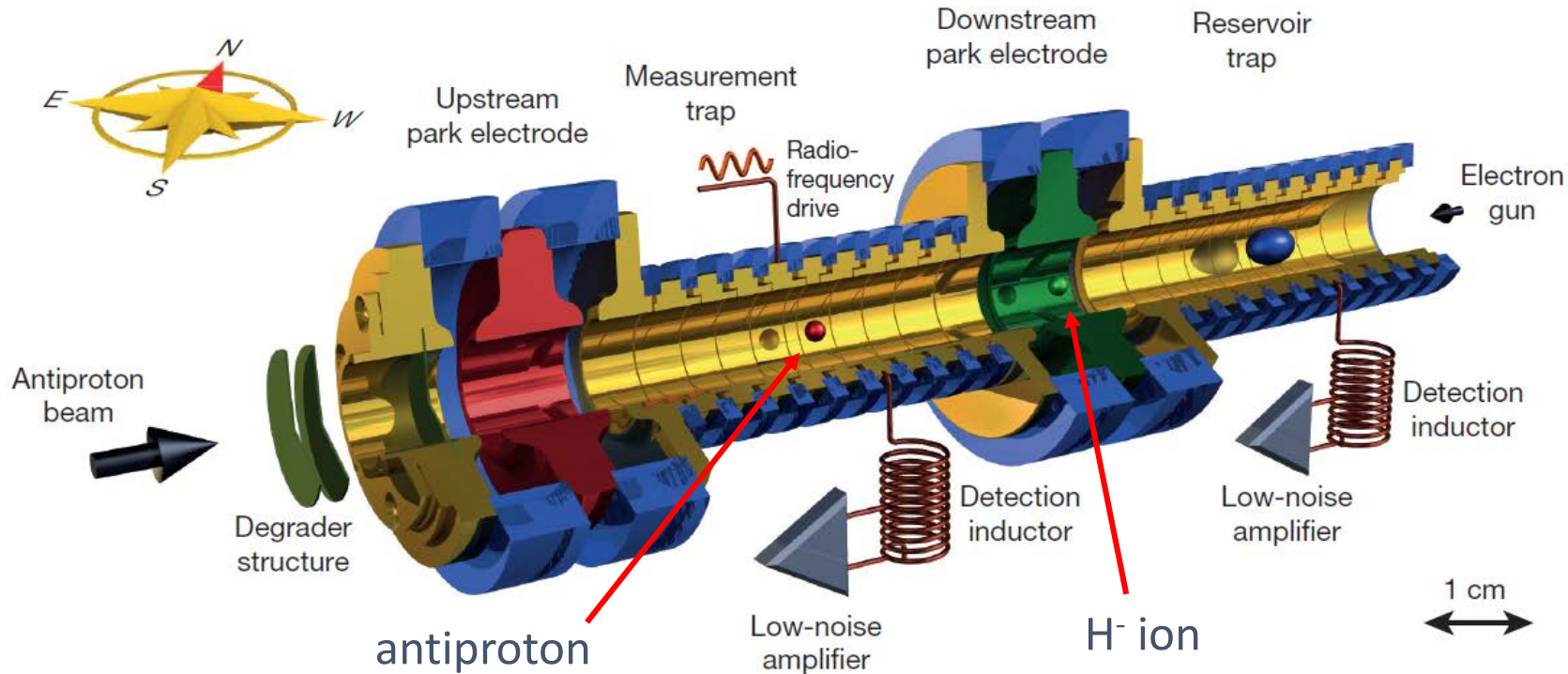
# Loading antiprotons and $H^-$ ions



- details of  $H^-$  trapping have yet to be understood.
- typical yield  $H^- / pbar = 1/3$ .
- managed to prepare a clean composite cloud of  $H^-$  and antiprotons.

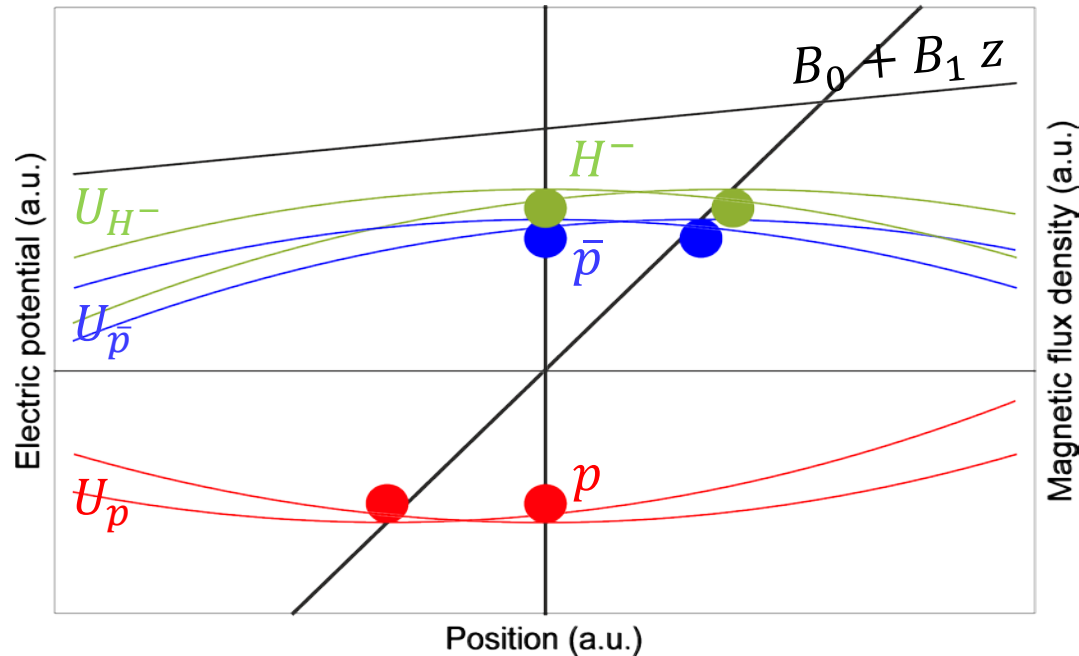
# Measurement configuration

Based on reservoir extraction technique and developed methods to prepare negative hydrogen ions we prepared an interesting set of initial conditions



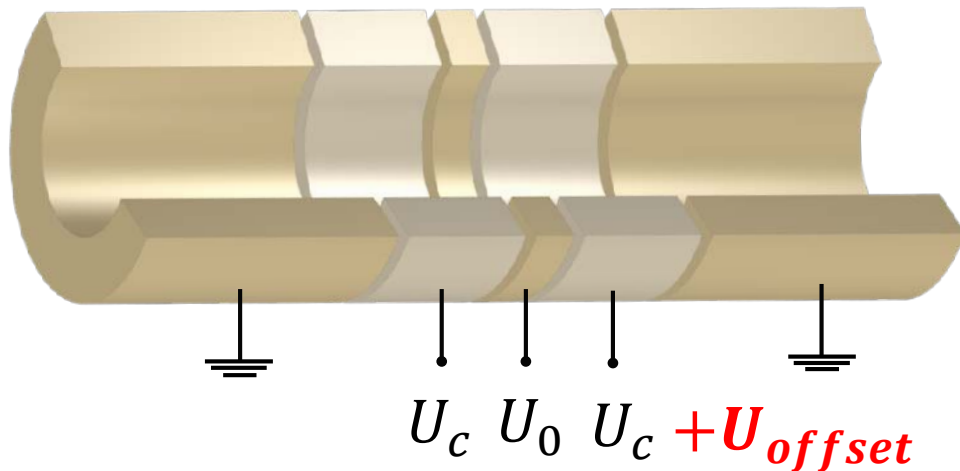
Comparison of H<sup>-</sup>/antiproton cyclotron frequencies:  
**One frequency ratio per 4 minutes with ~ 5 ppb uncertainty**

# Why not to use protons



- Systematic uncertainties due to the particle position are large ( $\sim 10^{-9}$ )
- No significant uncertainties in converting the mass ratio

$$\frac{m_{H^-}}{m_p} = \left( 1 + 2 \frac{m_e}{m_p} - \frac{E_b}{m_p} - \frac{E_a}{m_p} + \frac{\alpha_{\text{pol}, H^-} B_0^2}{m_p} \right)$$

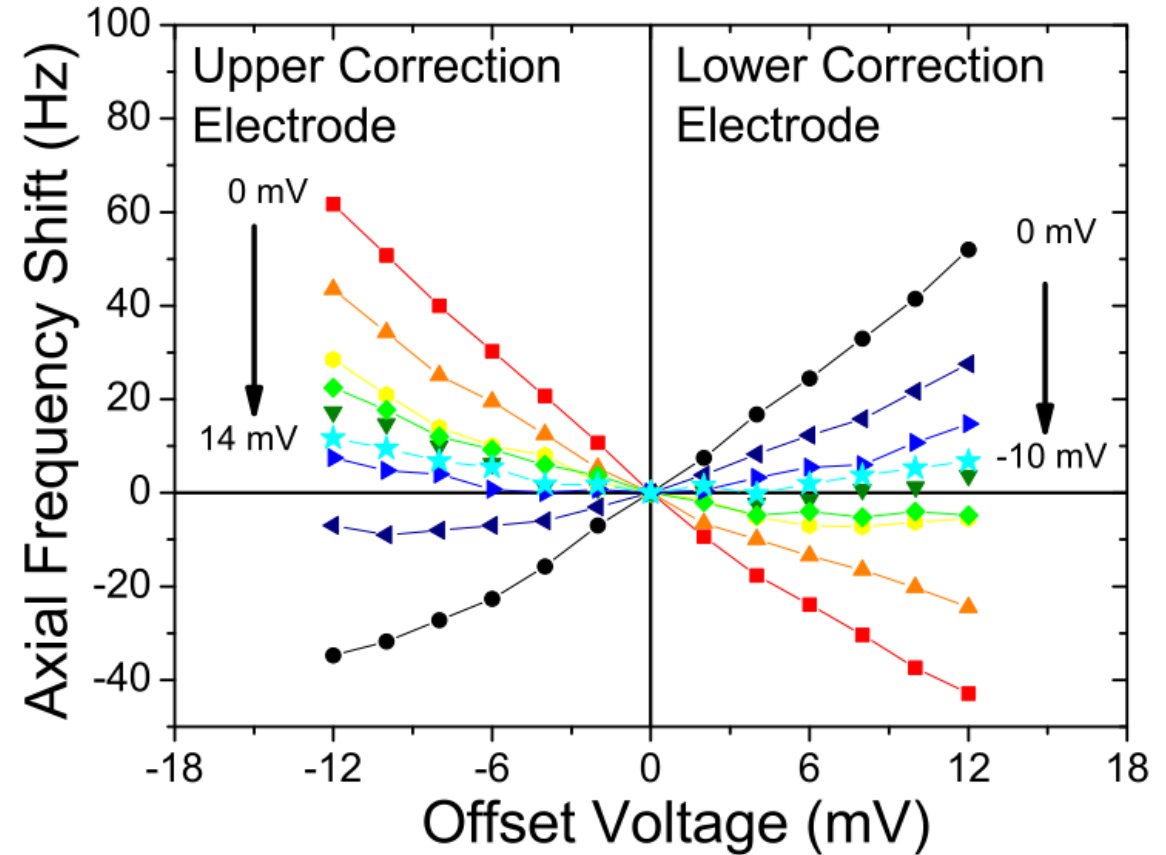


$$R_{\text{theo}} = 1.0010892187542(2) \quad (0.2 \text{ ppt})$$

- CPT test by a measurement of the cyclotron frequency ratio of antiproton and H<sup>-</sup> ion

# Asymmetry compensation

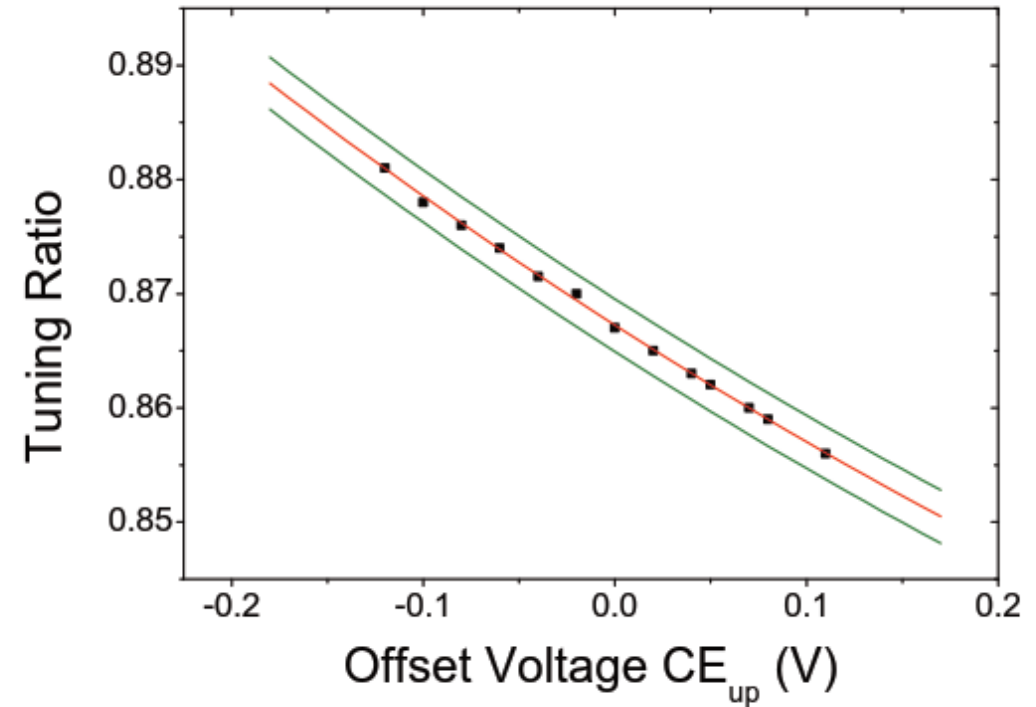
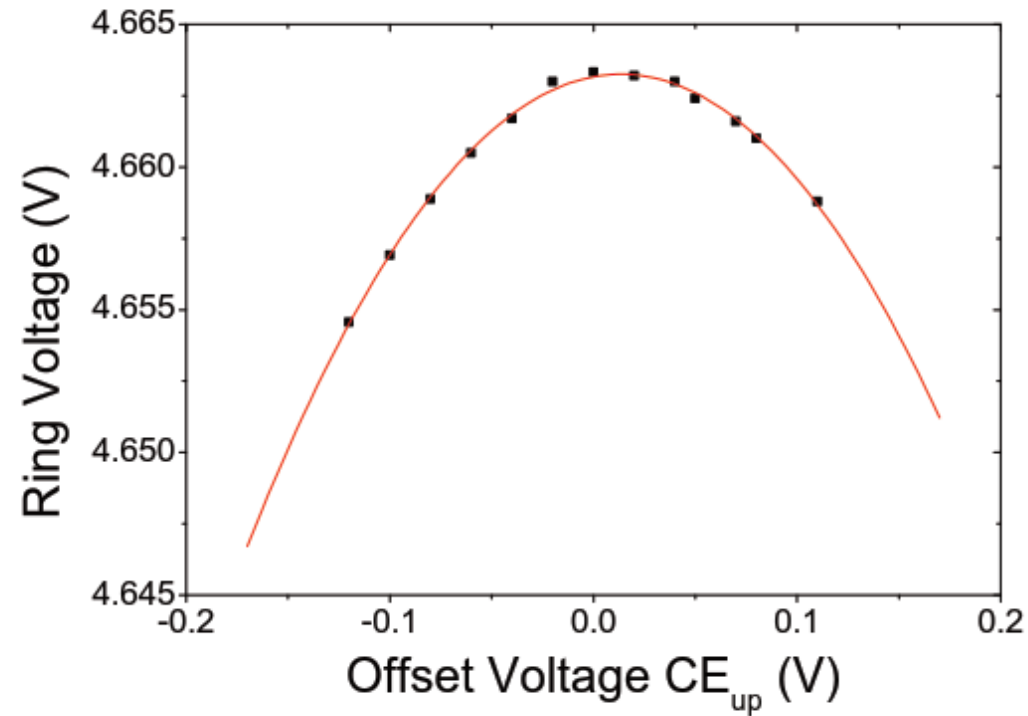
- The trap is symmetric if the potential on the correction electrodes (and endcaps) is identical
- The frequency shift induced by a voltage difference  $\Delta V$  applied to one correction electrode should be the same for both correction electrodes
- This allows to determine the offset potentials and compensate the voltage asymmetry
- The particle position becomes (more) independent from the ring voltage





# Trap geometry imperfections

Additional information on potential offsets and geometry imperfections can be learned from measuring the antiproton axial frequency for different voltage configurations:



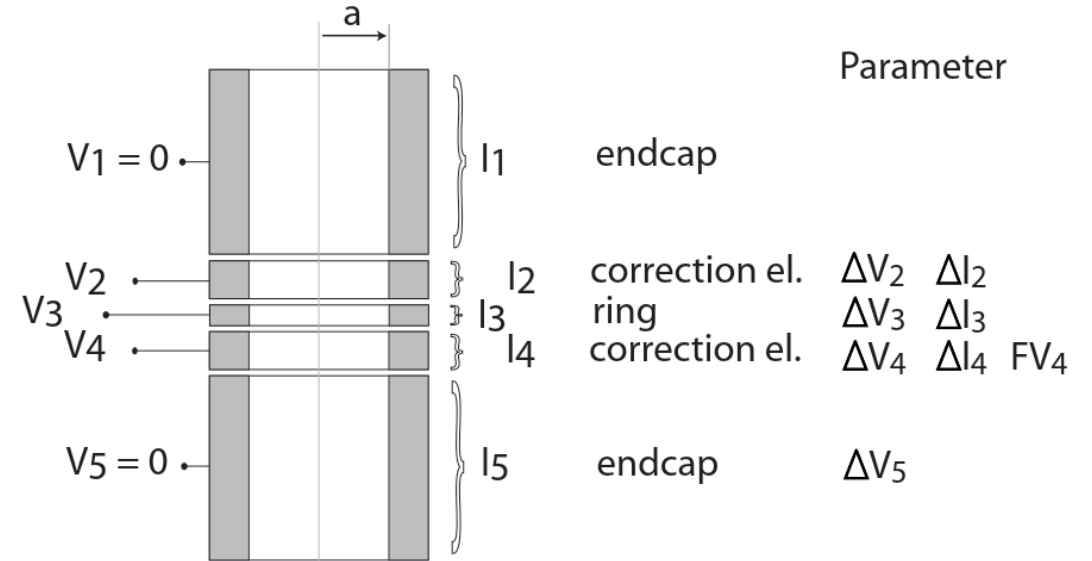


# Characterization of trap parameters

Comparing measurements and the trap coefficients from potential theory allows to determine the offset potentials and imperfections in the trap geometry:

$$C_j = \sum_{n=1}^{\infty} \left[ \frac{V_1 \cos(k_n z_0) - V_5 \cos(k_n \Lambda)}{k_n} + \sum_{i=1}^4 \frac{V_{i+1} - V_i}{k_n^2 d} \sin(k_n z_{2i}) - \sin(k_n z_{2i-1}) \right] \\ \times \frac{2}{j! \Lambda V_3} \left( \frac{n\pi}{\Lambda} \right)^j \frac{1}{I_0(k_n a)} \sin\left(\frac{\pi}{2}(n+j)\right) .$$

This allows to determine the position offset and the accompanied systematic shift.

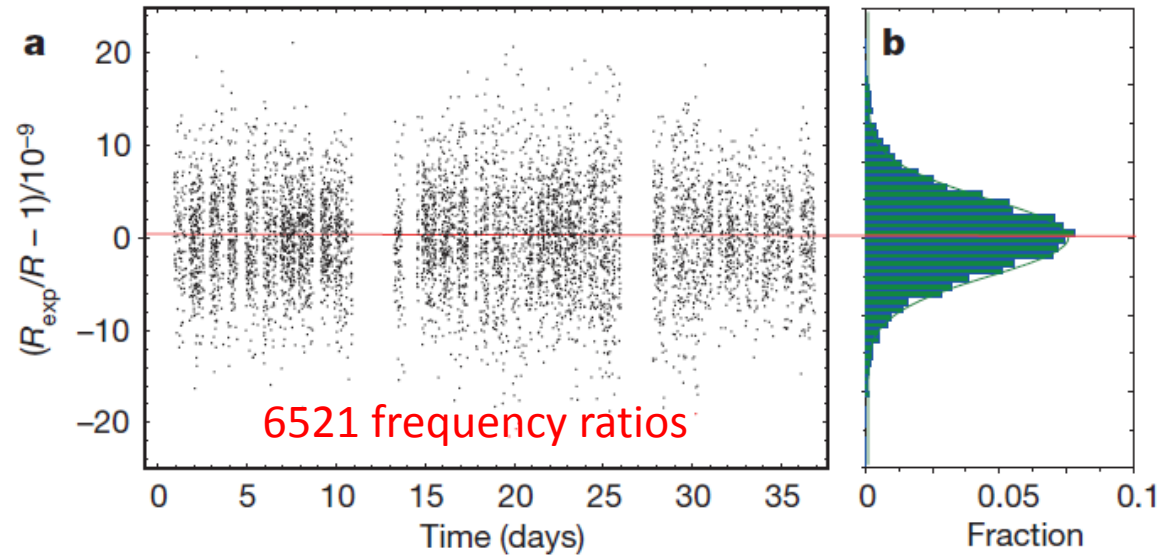


parameter	value	uncertainty	uncertainty in ratio shift in p.p.t.
$\Delta V_1$	0 mV	9 mV	9.9
$\Delta V_2$	-2 mV	5 mV	12.4
$\Delta V_3$	0 mV	7 mV	0.2
$\Delta V_4$	119 mV	1 mV	2.5
$\Delta V_5$	-10 mV	2 mV	2.2
$\Delta l_2$	18 $\mu\text{m}$	4 $\mu\text{m}$	4.7
$\Delta l_3$	29 $\mu\text{m}$	1 $\mu\text{m}$	1.1
$\Delta l_4$	0 $\mu\text{m}$	4 $\mu\text{m}$	4.7
$F_4$	0.985	0.002	19.8

# Other systematic uncertainties

	Effect	Shift (p.p.t.)	Uncertainty (p.p.t.)
$B_1$	Magnetic gradient shift	-0.002	0.0002
$B_2$	Magnetic bottle shift	0.009	0.012
$a$	Image charge shift	0.047	0.004
	Image current shift	<  0.001	<  0.001
$T_+$	Relativistic shift	-0.024	0.002
	Voltage drift	0.015	0.003
$\theta$	Tilt of apparatus	-0.027	0.007
	Rb-clock	–	3
$C_4$	Trap anharmonicity	3	1

# Data analysis and result



Width limited by random-walk noise of the magnetic field ( $\sim 5.5$  ppb)

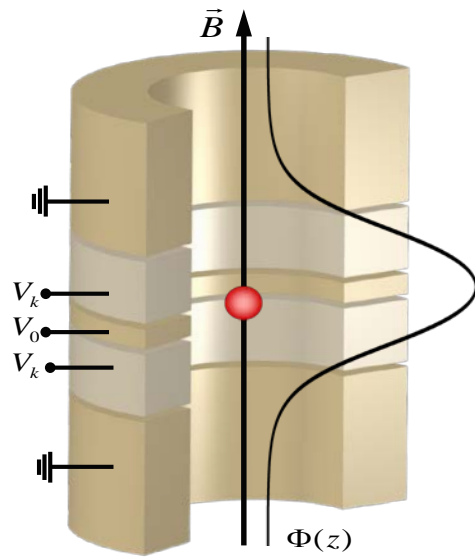
- Experimental result:

$$R_{\text{exp}} = 1.001\,089\,218\,872\,(64)$$

- Cyclotron frequency ratios for  $\bar{p}$ -to- $\bar{p}$  and  $\text{H}^-$ -to- $\text{H}^-$   $R_{\text{id}}$  are also evaluated

$$R_{\text{id}} - 1 = -3(79) \times 10^{-12} \leftarrow \text{Consistent with 1}$$

# Systematic Corrections



- Major systematic correction due to the residual magnetic B1 gradient.

- A displacement of 29 nm in the gradient of  $B1 = 7.6 \text{ mT / m}$  causes a correction of

$$dR_{B1} = -114(26) \text{ p.p.t.}$$

- Slight re-adjustment of the trapping potential:  $dR_{C4} = -3(1) \text{ p.p.t.}$

Final experimental result:

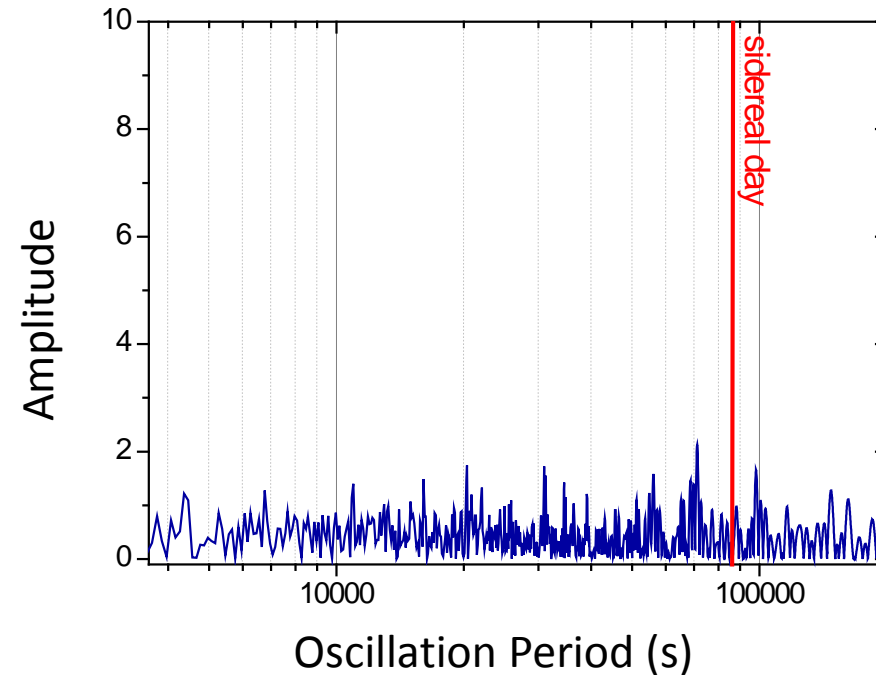
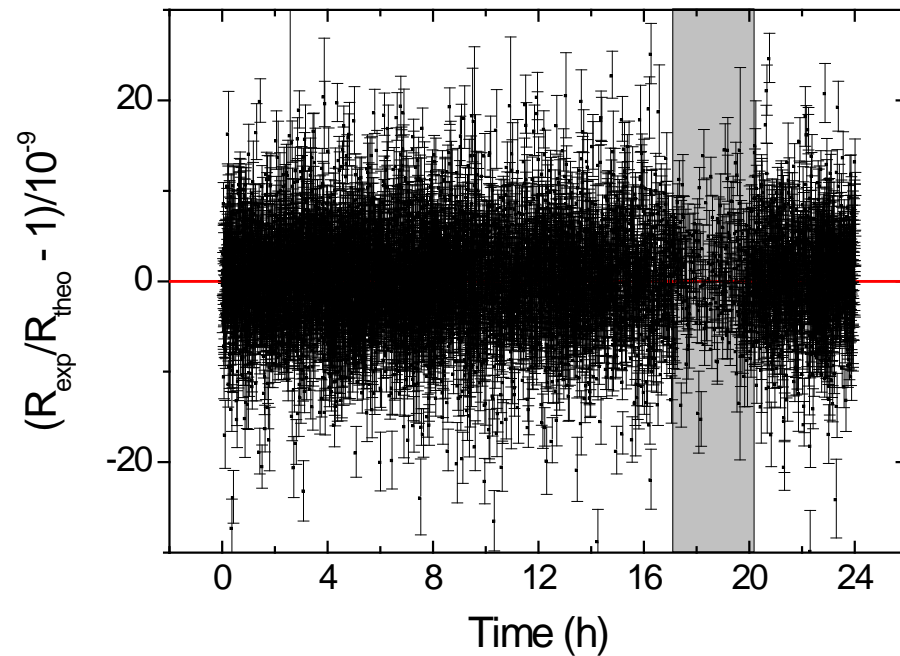
$$R_{\text{exp,c}} = 1.001\,089\,218\,755\,(64)\,(26)$$

$$\frac{(q/m)_{\bar{p}}}{(q/m)_p} + 1 = 1(69) \times 10^{-12}$$

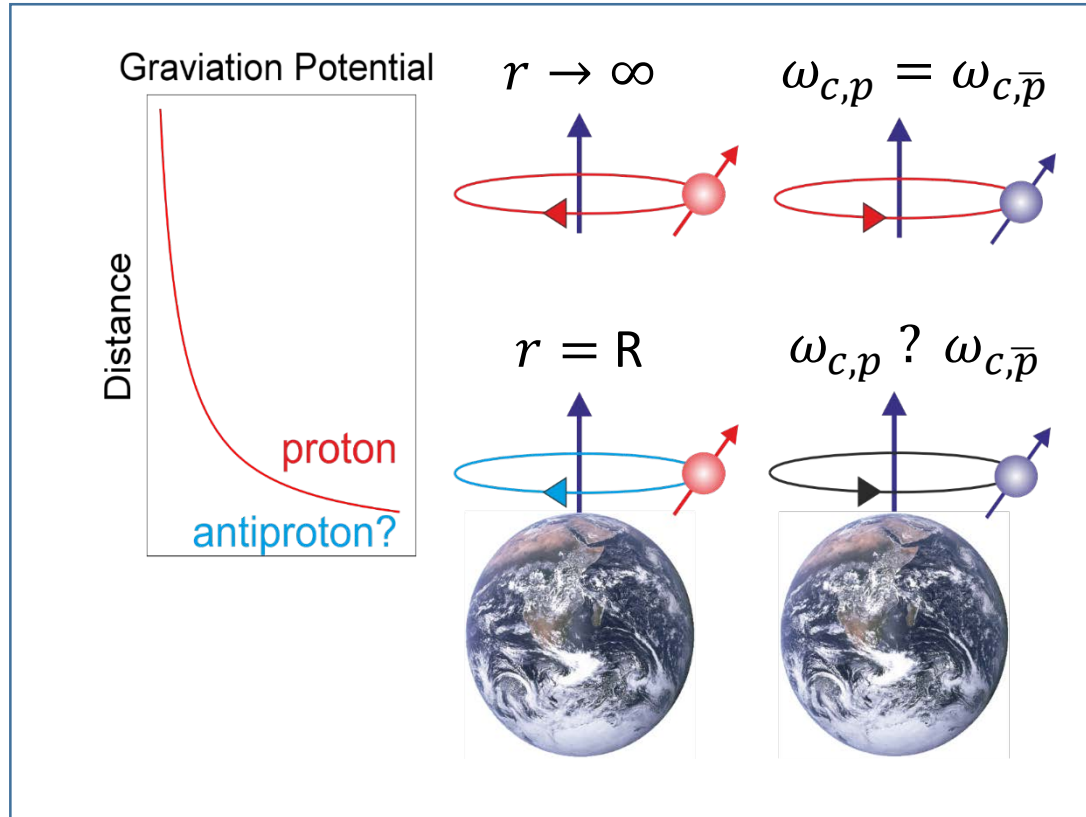
- In agreement with CPT conservation
- Exceeds the energy resolution of previous result by a factor of 4.

# Sidereal Variations (Lorentz violation)

- Constrains in first order CPT-even parameters of the Standard Model Extension
- Limit of sidereal variations in proton/antiproton charge-to-mass ratios to  $< 0.72$  ppb



# Antiproton gravitational redshift



- Cyclotron Frequency reflects the gravitational binding energy of the antiproton
- Gravitational anomaly can be constrained

$$\frac{\omega_{c,p} - \omega_{c,\bar{p}}}{\omega_{c,p}} = -3(\alpha_g - 1) U/c^2$$

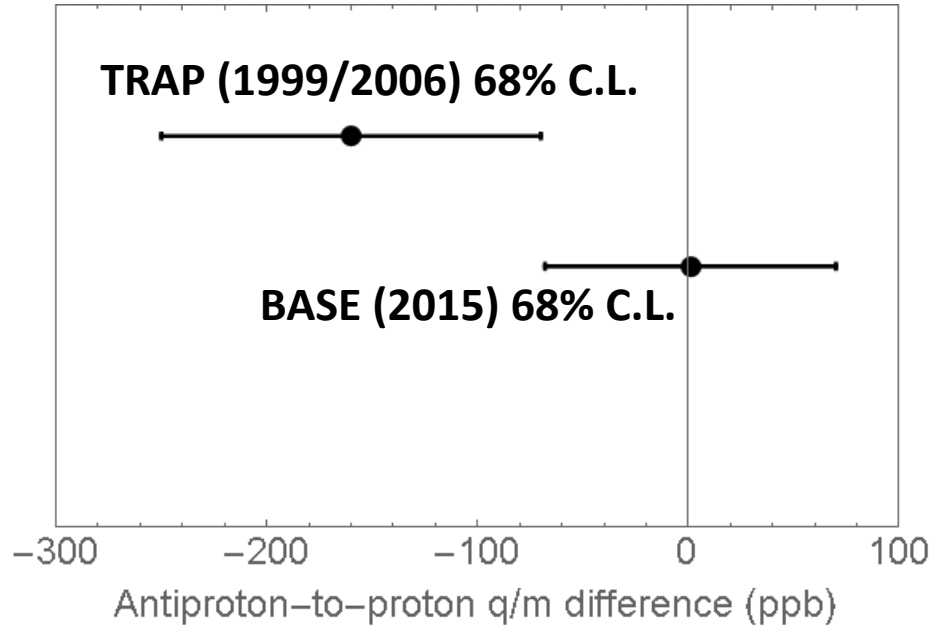
Our 69ppt result sets  
a new upper limit of

$$|\alpha_g - 1| < 8.7 \times 10^{-7}$$

S. Ulmer et al., *Nature* **524** 196 (2015)

- Cyclotron frequency ratio depends on (q/m)-difference, SME-coefficients, and the gravitational anomaly
- Limits on the gravitational anomaly depend on assumptions on the gravitation potential U

# Conclusions to antiproton Q/M



Most precise comparison of a fundamental quantity of baryons and antibaryons.

Test of the standard model with  $h\Delta\nu_c = 8 \cdot 10^{-18}$  eV energy resolution.

Factor 4 improvement in energy resolution due to lower cyclotron frequency

Limitations due to the magnetic field fluctuations have been improved

A more precise measurement seems feasible

